Cloud Detection

Rennan Marujo

2019-Oct-03

Cloud coverage - CBERS-4 from November to December/2018

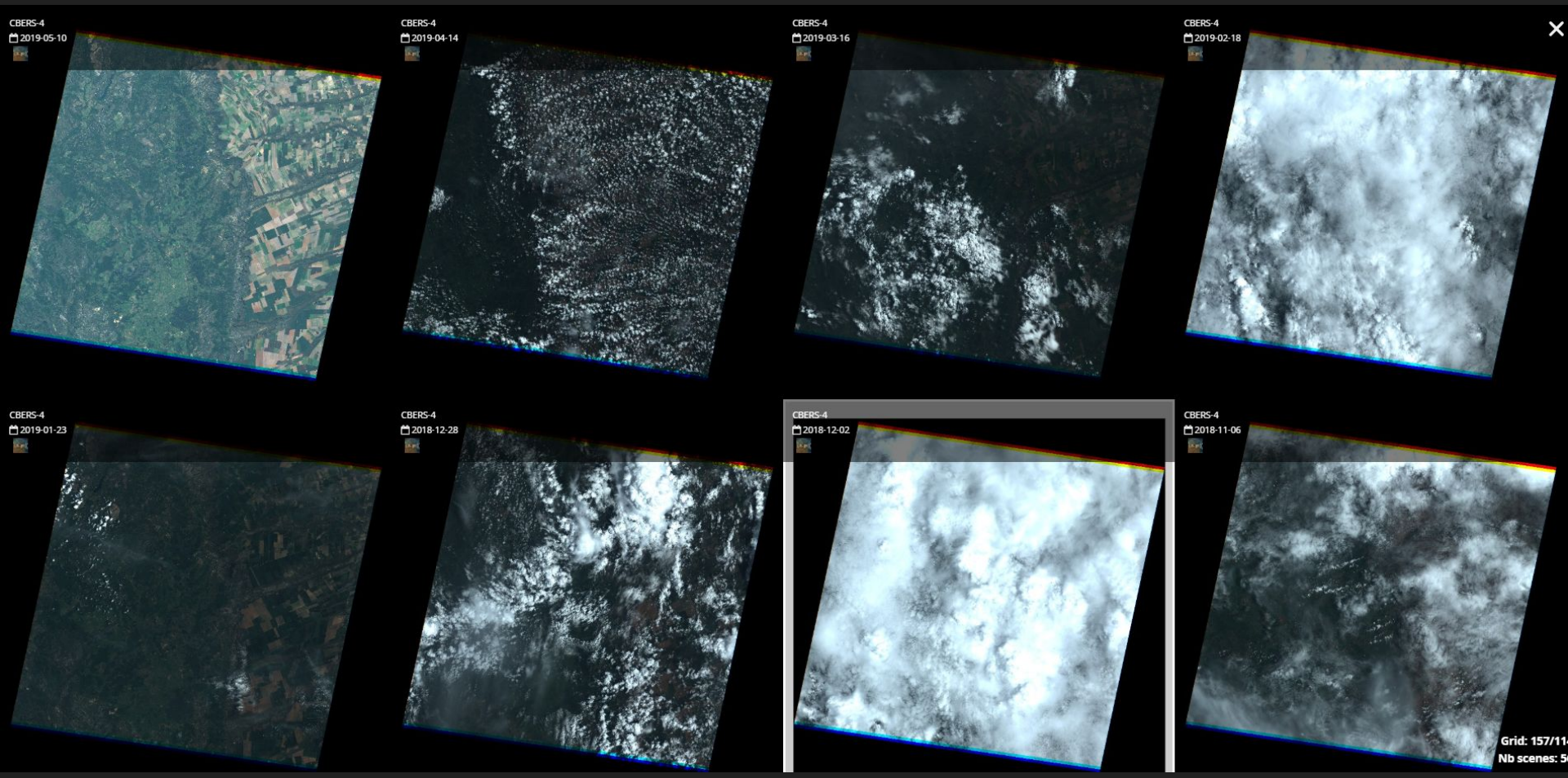

Source: https://search.remotepixel.ca/#3/-29.56/-51.39

Cloud coverage - Landsat-8 from November to December/2018

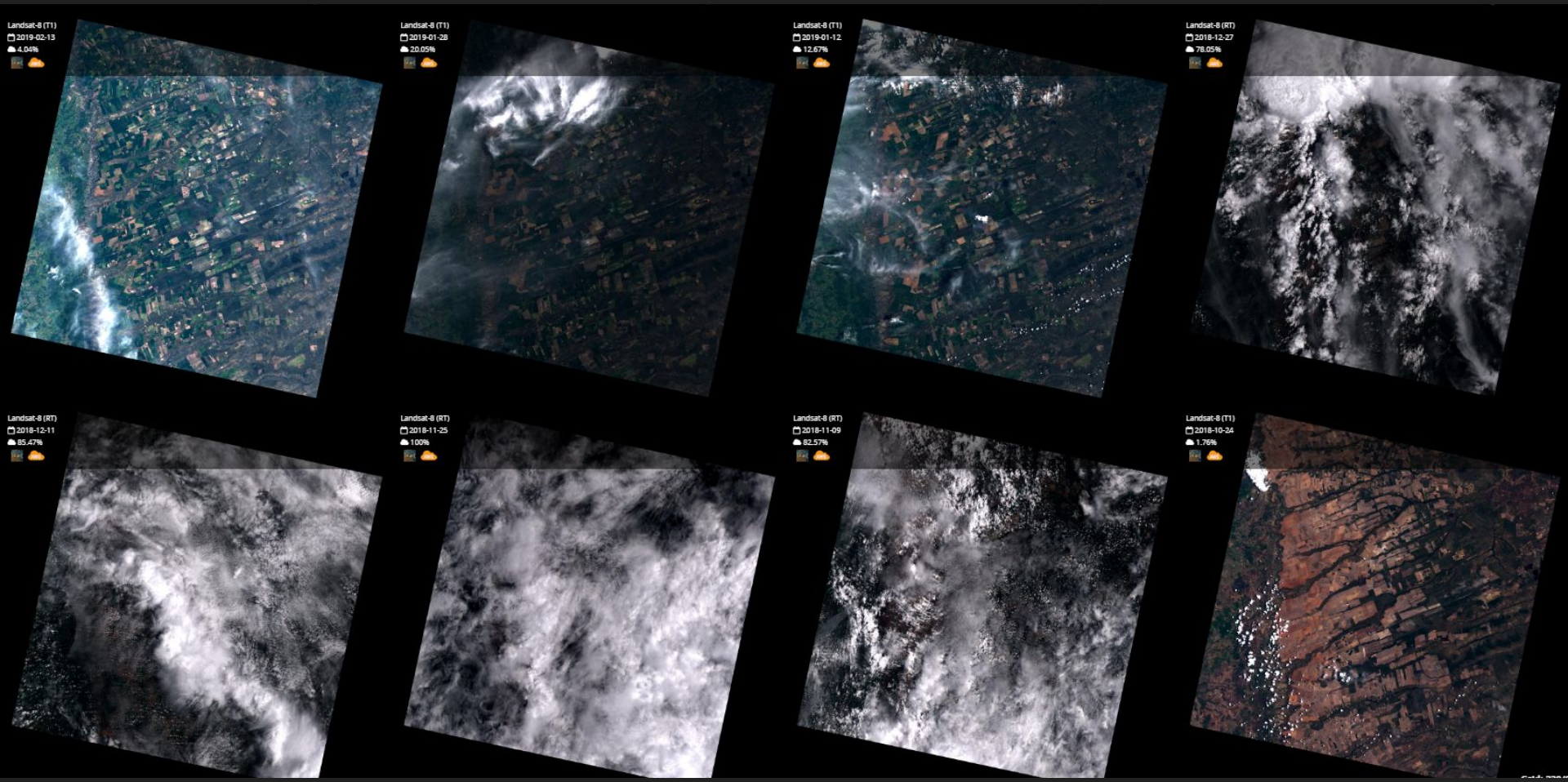

Source: https://search.remotepixel.ca/#3/-29.56/-51.39

Cloud coverage - Sentinel-2 from November to December/2018

Source: https://search.remotepixel.ca/#3/-29.56/-51.39

2. Cloud Detection

1

Cloud and Cloud Shadow Detection for Landsat Images: The Fundamental Basis for Analyzing Landsat Time Series

Zhe Zhu, Shi Qiu, Binbin He, and Chengbin Deng

CONTENTS

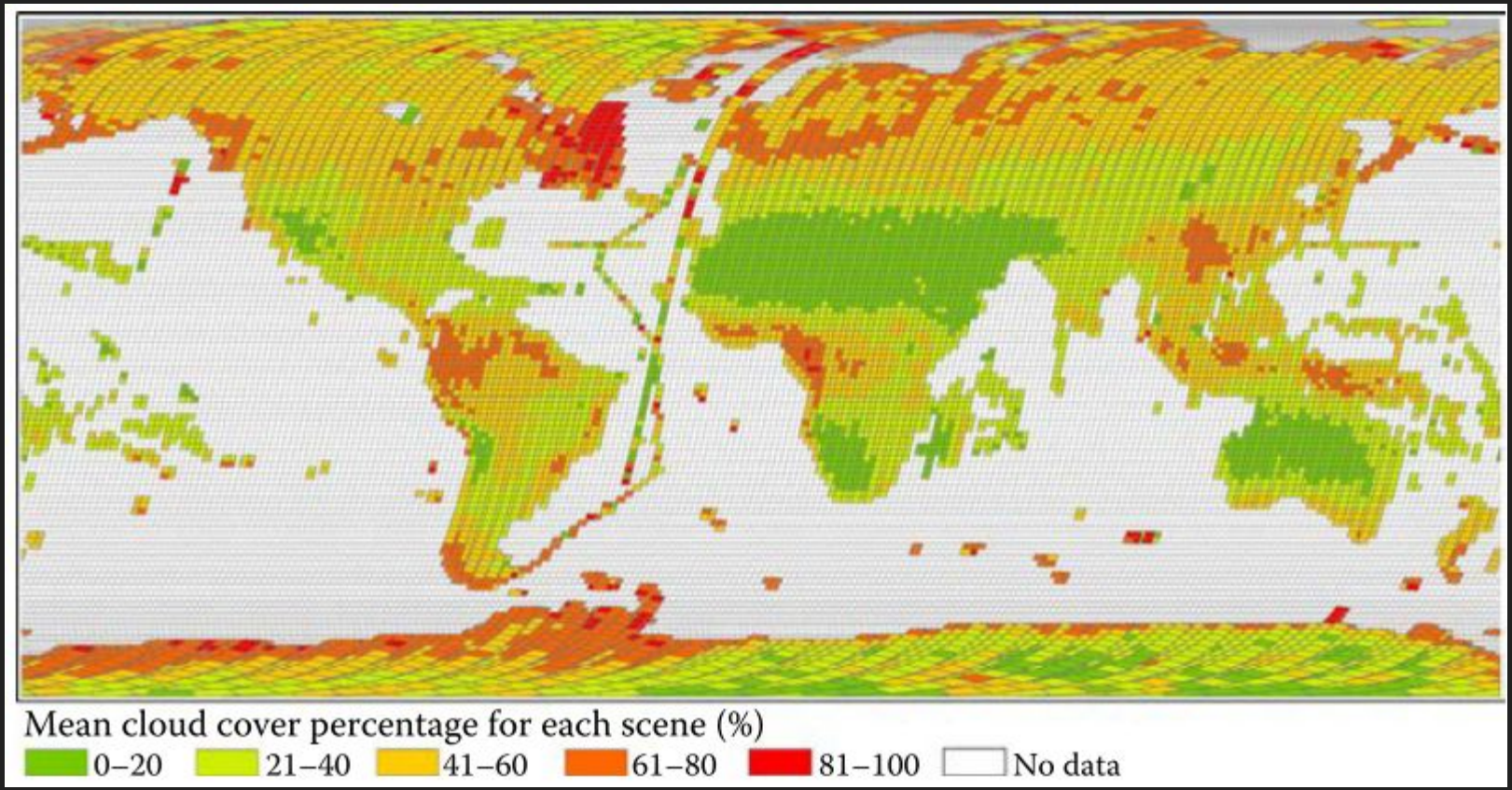

Zhu et. al (2018)

Manual Cloud and Cloud Shadow Masks Derived from Landsat Images

Name	Sensor	Number of Images	Date Range		Error	Reference
			Start	End		
L7 Irish	ETM+ (SLC on)	206 (45)	06/06/2000	12/30/2001	7.00%	USGS (2016a)
L8 SPARCS	OLI	80 (80)	05/12/2013	11/02/2014	4.00%	USGS (2016b)
L8 Biome	OLI	96 (33)	04/13/2013	11/05/2014	Less than 7.00%	USGS (2016c)

Zhu et. al (2018)

Manual Cloud and Cloud Shadow Masks Derived from Landsat Images

Name	Sensor	Number of Images	Date Range		Error	Reference
			Start	End		
L7 Irish	ETM+ (SLC on)	206 (45)	06/06/2000	12/30/2001	7.00%	USGS (2016a)
L8 SPARCS	OLI	80 (80)	05/12/2013	11/02/2014	4.00%	USGS (2016b)
L8 Biome	OLI	96 (33)	04/13/2013	11/05/2014	Less than 7.00%	USGS (2016c)

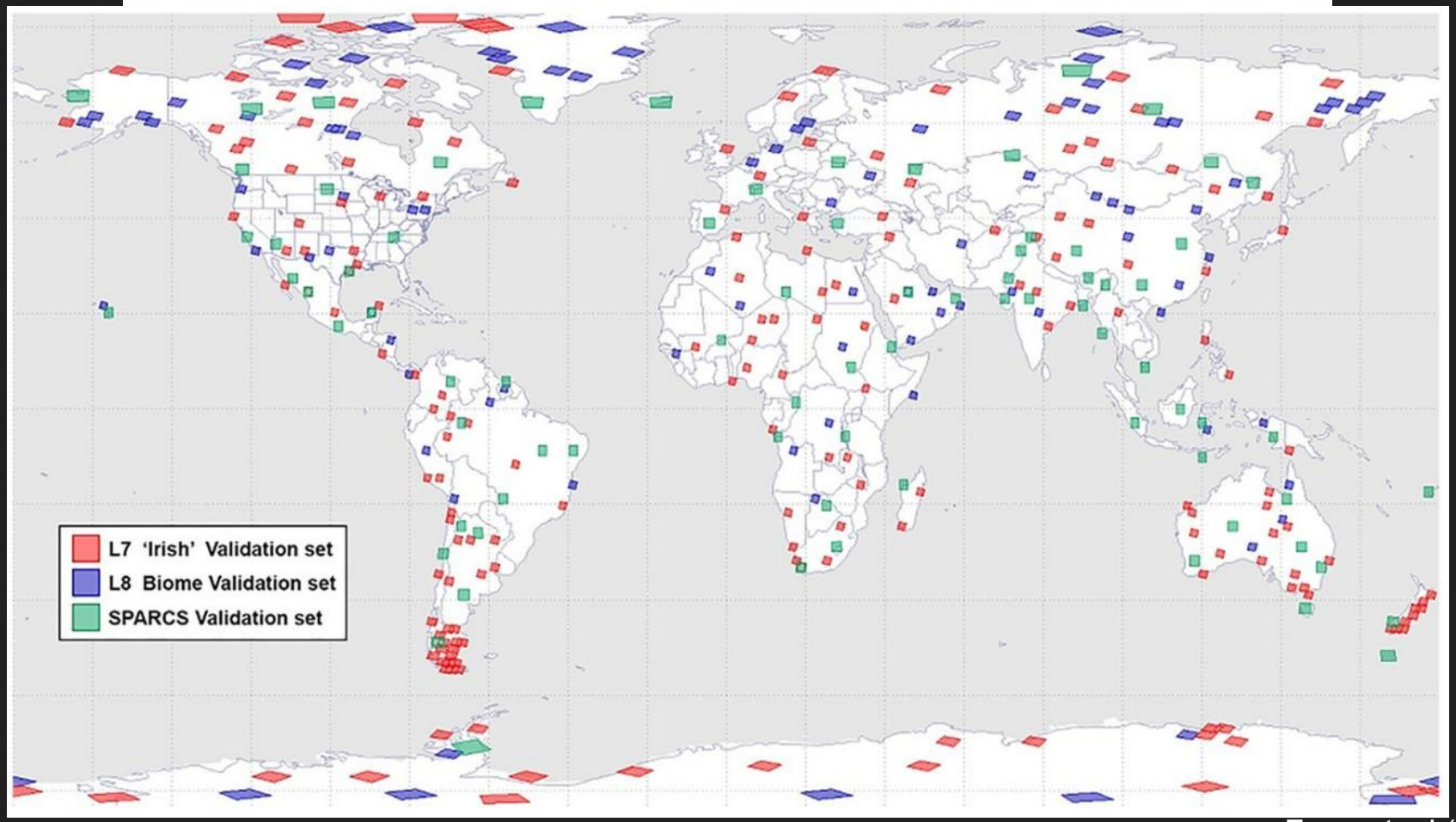

Foga et. al (2017)

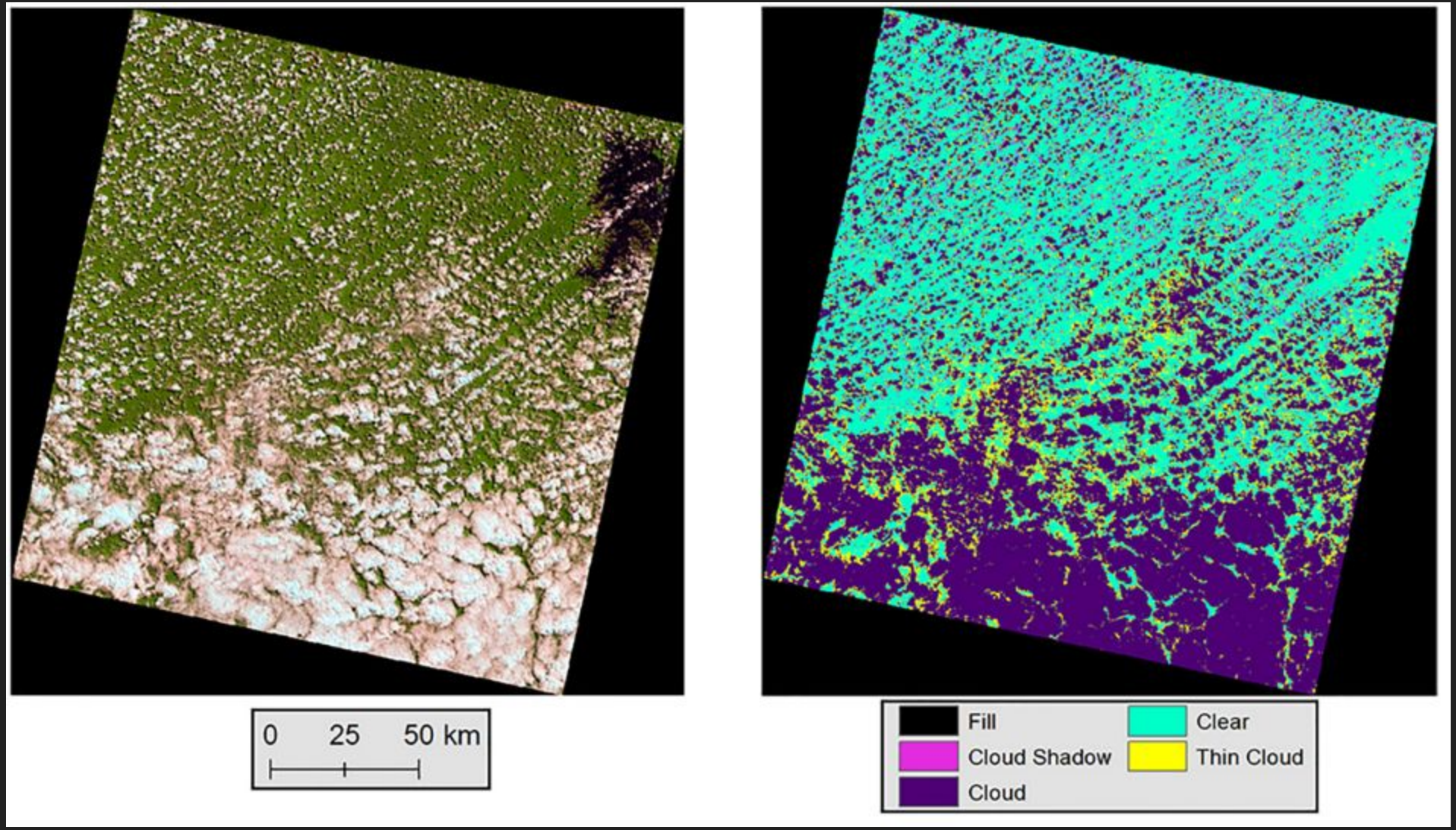

Foga et. al (2017)

Challenges

Cloud
Snow/ice
building top
beaches
sand dunes
salt lakes

Cloud Shadow
Water
wetlands
dark urban
terrain shadow

Landsat 1–5 MSS, Landsat 4–5 TM, Landsat 7 ETM+ and Landsat 8 OLI Sensor Characteristics

Landsat 1–5 MSS Bands (μm)	Landsat 4–5 TM Bands (μm)	Landsat 7 ETM+ Bands (μm)	Landsat 8 OLI/TIRS Bands (μm)
	Band 1 (0.45–0.52)	Band 1 (0.45–0.52)	Band 1 (0.435–0.451)
Band 4 (0.50–0.60)	Band 2 (0.52–0.60)	Band 2 (0.52–0.60)	Band 2 (0.452–0.512)
Band 5 (0.60–0.70)	Band 3 (0.63–0.69)	Band 3 (0.63–0.69)	Band 3 (0.533–0.590)
Band 6 (0.70–0.80)	Band 4 (0.76–0.90)	Band 4 (0.77–0.90)	Band 4 (0.636–0.673)
Band 7 (0.80–1.10)			
	Band 5 (1.55–1.75)	Band 5 (1.55–1.75)	Band 5 (0.851–0.879)
Band 8 (10.40–12.50) Landsat 3 only[a]	Band 6 (10.40–12.50)	Band 6 (10.40–12.50)	Band 6 (1.566–1.651)
	Band 7 (2.08–2.35)	Band 7 (2.09–2.35)	Band 7 (2.107–2.294)
		Band 8 (0.52–0.90)	Band 8 (0.503–0.676)
			Band 9 (1.363–1.384)
			Band 10 (10.60–11.19)
			Band 11 (11.50–12.51)

[a] Indicates that the thermal band of the Landsat 3 MSS was unsuccessful and not available.

Zhu et. al (2018)

Characteristics of Different Cloud and Cloud Shadow Detection Algorithms for Landsat Images

Category
Single-date:
Multi-date

Zhu et. al (2018)

Characteristics of Different Cloud and Cloud Shadow Detection Algorithms for Landsat Images

Category
Single-date: Physical rules
Single-date: Machine learning
Multi-date

Zhu et. al (2018)

Characteristics of Different Cloud and Cloud Shadow Detection Algorithms for Landsat Images

Category	Algorithm Name	Landsat Sensor	Cloud/ Shadow	Ancillary Data	Overall Accuracy	Reference
Single-date: Physical rules	MFmask	TM ETM+ OLI/TIRS	Both	DEM	96%	Qiu et al. (2017)
	LSR 8	OLI/TIRS	Both	N/A	N/A	Vermote et al. (2016)
	UDTCDA	OLI/TIRS	Cloud	MOD09A1	N/A	Sun et al. (2016)
	MSScvm	MSS	Both	DEM	84%	Braaten et al. (2015)
	ELTK	OLI/TIRS	Cloud	N/A	N/A	Wilson and Oreopoulos (2013)
	Fmask	TM ETM+ OLI/TIRS	Both	N/A	96%	Zhu and Woodcock (2012), Zhu et al. (2015)
	N/A	TM ETM+	Both	DEM	88%~99%	Huang et al. (2010)
	LTK	TM ETM+ OLI/TIRS	Cloud	N/A	93%	Oreopoulos et al. (2011)
	LEDAPS	TM ETM+	Both	Air temperature from NCEP	N/A	Vermote and Saleous (2007)
	CDSM/ANTD	ETM+	Both	N/A	N/A	Choi and Bindschadler (2004)
	ACCA	TM ETM+ OLI/TIRS	Cloud	N/A	N/A	Irish (2000), Irish et al. (2006)
Single-date: Machine learning	N/A	OLI	Cloud	N/A	N/A	Zhou et al. (2016)
	SPARCS	ETM+	Both	N/A	99%	Hughes and Hayes (2014)
	See5	OLI	Cloud	N/A	89%	Scaramuzza et al. (2012)
	AT-ACCA	OLI	Cloud	N/A	90%	Scaramuzza et al. (2012)
	N/A	ETM+	Both	N/A	N/A	Potapov et al. (2011)
	N/A	ETM+	Cloud	N/A	N/A	Roy et al. (2010)
	N/A	MSS	Cloud	N/A	93%	Lee et al. (1990)
Multi-date	IHOT	MSS TM ETM+	Cloud	N/A	N/A	Chen et al. (2015)
	Tmask[a]	TM ETM+ OLI/TIRS	Both	N/A	N/A	Zhu and Woodcock (2014)
	N/A[a]	TM ETM+	Both	N/A	97%	Goodwin et al. (2013)
	N/A	TM ETM+	Both	N/A	N/A	Jin et al. (2013)
	MTCD[a]	TM ETM+	Both	Sentinel-2 data	N/A	Hagolle et al. (2010)
	N/A	TM	Both	N/A	N/A	Wang et al. (1999)

Zhu et. al (2018)

Characteristics of Different Cloud and Cloud Shadow Detection Algorithms for Landsat Images

Category	Algorithm Name	Landsat Sensor	Cloud/ Shadow	Ancillary Data	Overall Accuracy	Reference
Single-date: Physical rules	MFmask	TM ETM+ OLI/TIRS	Both	DEM	96%	Qiu et al. (2017)
	LSR 8	OLI/TIRS	Both	N/A	N/A	Vermote et al. (2016)
	UDTCDA	OLI/TIRS	Cloud	MOD09A1	N/A	Sun et al. (2016)
	MSScvm	MSS	Both	DEM	84%	Braaten et al. (2015)
	ELTK	OLI/TIRS	Cloud	N/A	N/A	Wilson and Oreopoulos (2013)
	Fmask	TM ETM+ OLI/TIRS	Both	N/A	96%	Zhu and Woodcock (2012), Zhu et al. (2015)
	N/A	TM ETM+	Both	DEM	88%~99%	Huang et al. (2010)
	LTK	TM ETM+ OLI/TIRS	Cloud	N/A	93%	Oreopoulos et al. (2011)
	LEDAPS	TM ETM+	Both	Air temperature from NCEP	N/A	Vermote and Saleous (2007)
	CDSM/ANTD	ETM+	Both	N/A	N/A	Choi and Bindschadler (2004)
	ACCA	TM ETM+ OLI/TIRS	Cloud	N/A	N/A	Irish (2000), Irish et al. (2006)
Single-date: Machine learning	N/A	OLI	Cloud	N/A	N/A	Zhou et al. (2016)
	SPARCS	ETM+	Both	N/A	99%	Hughes and Hayes (2014)
	See5	OLI	Cloud	N/A	89%	Scaramuzza et al. (2012)
	AT-ACCA	OLI	Cloud	N/A	90%	Scaramuzza et al. (2012)
	N/A	ETM+	Both	N/A	N/A	Potapov et al. (2011)
	N/A	ETM+	Cloud	N/A	N/A	Roy et al. (2010)
	N/A	MSS	Cloud	N/A	93%	Lee et al. (1990)
Multi-date	IHOT	MSS TM ETM+	Cloud	N/A	N/A	Chen et al. (2015)
	Tmask[a]	TM ETM+ OLI/TIRS	Both	N/A	N/A	Zhu and Woodcock (2014)
	N/A[a]	TM ETM+	Both	N/A	97%	Goodwin et al. (2013)
	N/A	TM ETM+	Both	N/A	N/A	Jin et al. (2013)
	MTCD[a]	TM ETM+	Both	Sentinel-2 data	N/A	Hagolle et al. (2010)
	N/A	TM	Both	N/A	N/A	Wang et al. (1999)

Zhu et. al (2018)

Characteristics of Different Cloud and Cloud Shadow Detection Algorithms for Landsat Images

Category	Algorithm Name	Landsat Sensor	Cloud/ Shadow	Ancillary Data	Overall Accuracy	Reference
Single-date: Physical rules	MFmask	TM ETM+ OLI/TIRS	Both	DEM	96%	Qiu et al. (2017)
	LSR 8	OLI/TIRS	Both	N/A	N/A	Vermote et al. (2016)
	UDT(					t al. (2016)
	MSSc					en et al. (2015)
	ELTK					n and Oreopoulos 3)
	Fmas					and Woodcock (2012), et al. (2015)
	N/A					g et al. (2010)
	LTK					poulos et al. (2011)
	LED/					ote and Saleous (2007)
	CDSM					and Bindschadler (2004)
	ACC.					(2000), Irish et al. (2006)
Single-date: Machine learning	N/A					et al. (2016)
	SPAR					es and Hayes (2014)
	See5					muzza et al. (2012)
	AT-A					muzza et al. (2012)
	N/A					ov et al. (2011)
	N/A					t al. (2010)
	N/A	MSS	Cloud	N/A	93%	Lee et al. (1990)
Multi-date	IHOT	MSS TM ETM+	Cloud	N/A	N/A	Chen et al. (2015)
	Tmask[a]	TM ETM+ OLI/TIRS	Both	N/A	N/A	Zhu and Woodcock (2014)
	N/A[a]	TM ETM+	Both	N/A	97%	Goodwin et al. (2013)
	N/A	TM ETM+	Both	N/A	N/A	Jin et al. (2013)
	MTCD[a]	TM ETM+	Both	Sentinel-2 data	N/A	Hagolle et al. (2010)
	N/A	TM	Both	N/A	N/A	Wang et al. (1999)

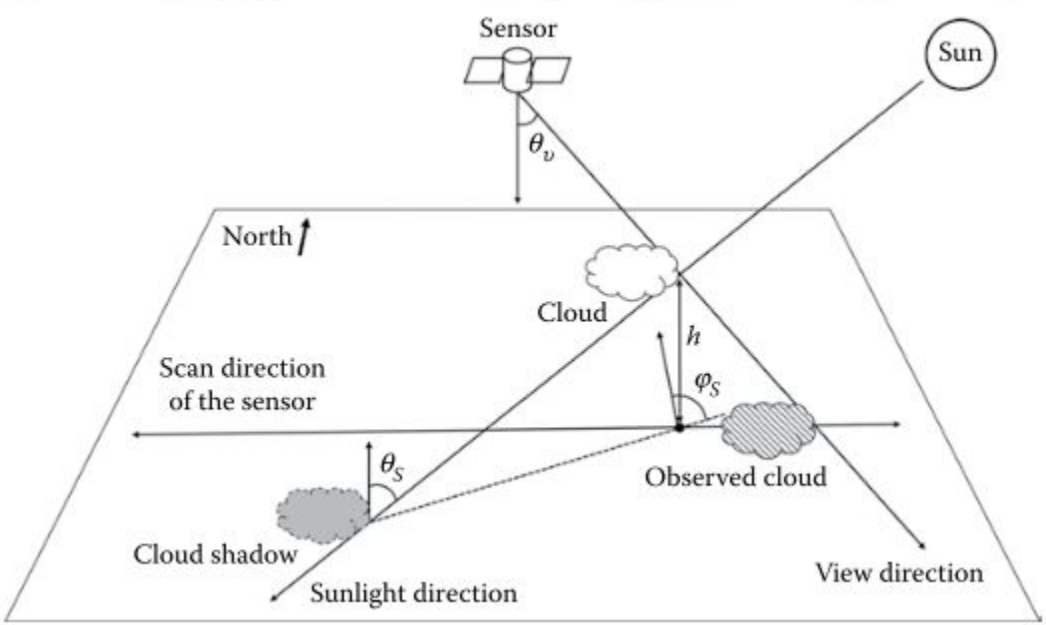

Richter et. al (2012)

Characteristics of Different Cloud and Cloud Shadow Detection Algorithms for Landsat Images

Category	Algorithm Name	Landsat Sensor	Cloud/ Shadow	Ancillary Data	Overall Accuracy	Reference
Single-date: Physical rules	MFmask	TM ETM+ OLI/TIRS	Both	DEM	96%	Qiu et al. (2017)
	LSR 8	OLI/TIRS	Both	N/A	N/A	Vermote et al. (2016)
	UDTCDA	OLI/TIRS	Cloud	MOD09A1	N/A	Sun et al. (2016)
	MSScvm	MSS	Both	DEM	84%	Braaten et al. (2015)
	ELTK	OLI/TIRS	Cloud	N/A	N/A	Wilson and Oreopoulos (2013)
	Fmask	TM ETM+ OLI/TIRS	Both	N/A	96%	Zhu and Woodcock (2012), Zhu et al. (2015)
	N/A	TM ETM+	Both	DEM	88%~99%	Huang et al. (2010)
	LTK	TM ETM+ OLI/TIRS	Cloud	N/A	93%	Oreopoulos et al. (2011)
	LEDAPS	TM ETM+	Both	Air temperature from NCEP	N/A	Vermote and Saleous (2007)
	CDSM/ANTD	ETM+	Both	N/A	N/A	Choi and Bindschadler (2004)
	ACCA	TM ETM+ OLI/TIRS	Cloud	N/A	N/A	Irish (2000), Irish et al. (2006)
Single-date: Machine learning	N/A	OLI	Cloud	N/A	N/A	Zhou et al. (2016)
	SPARCS	ETM+	Both	N/A	99%	Hughes and Hayes (2014)
	See5	OLI	Cloud	N/A	89%	Scaramuzza et al. (2012)
	AT-ACCA	OLI	Cloud	N/A	90%	Scaramuzza et al. (2012)
	N/A	ETM+	Both	N/A	N/A	Potapov et al. (2011)
	N/A	ETM+	Cloud	N/A	N/A	Roy et al. (2010)
	N/A	MSS	Cloud	N/A	93%	Lee et al. (1990)
Multi-date	IHOT	MSS TM ETM+	Cloud	N/A	N/A	Chen et al. (2015)
	Tmask[a]	TM ETM+ OLI/TIRS	Both	N/A	N/A	Zhu and Woodcock (2014)
	N/A[a]	TM ETM+	Both	N/A	97%	Goodwin et al. (2013)
	N/A	TM ETM+	Both	N/A	N/A	Jin et al. (2013)
	MTCD[a]	TM ETM+	Both	Sentinel-2 data	N/A	Hagolle et al. (2010)
	N/A	TM	Both	N/A	N/A	Wang et al. (1999)

Zhu et. al (2018)

CFmask
Landsat Ecosystem Disturbance Adaptive Processing System (LEDAPS)

LEDAPS surface reflectance product description

Version 2.0, January 2007

Top of the atmosphere reflectance in Red (band 3), Green (band 2), Blue (band 1) of Landsat ETM+

LEDAPS Surface reflectance in Red (band 3), Green (band 2), Blue (band 1) of Landsat ETM+

Eric Vermote

$$WT=(NDVI < 0.1) \; OR \; (\rho(band\ 4) < 0.04 \; AND \; \rho(band\ 5) < 0.05))$$

Water test

Vermote et. al (2007)

$$WT=(NDVI < 0.1)\ OR\ (\ \rho(band\ 4) < 0.04\ AND\ \rho(band\ 5) < 0.05)\ )$$

Water test

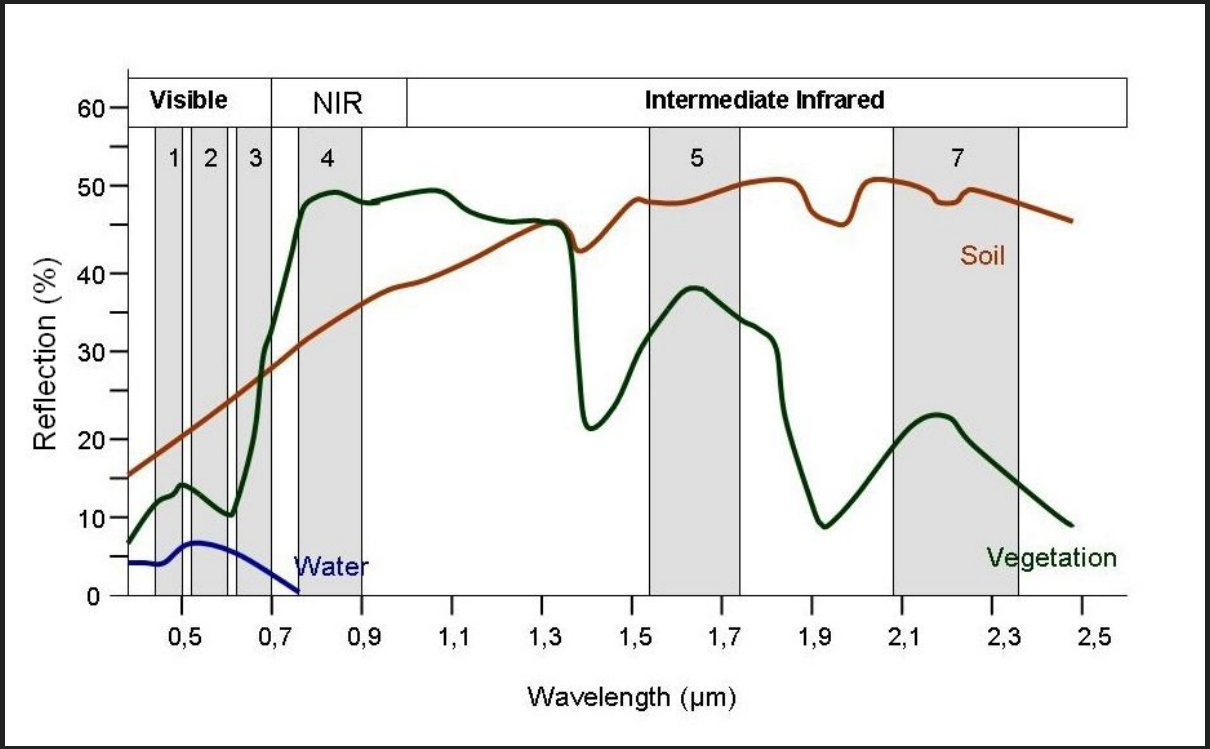

Cloud test

$$VRAT = (\rho^s(blue=band1) - 0.5.\rho^s(Red=band3)) > 0.08$$

BTT=Brightness Temperature (Band 6) < Air temp(NCEP)-20 [Degree Celsius]

$$RT = \rho^s(band\ 3) > 0.4 \text{ or } \rho^s(band\ 4) > 0.6$$

$$SRT = 0.9 < (\rho^s(band\ 4) / \rho^s(band\ 3)) < 1.3$$

Another test is also added to reject any possible unfiltered water pixel or pixel contaminated by shadow, it uses the band 7 reflectance and requires that the selected pixels have a reflectance > 0.03.

Vermote et. al (2007)

The reflectance in band 7 is greater than 0.03 AND
a) The brightness temperature of this pixel is lower than the final air temperature threshold
OR
b) If it is brightness temperature is lower than the air temperature threshold by no more than 4 degree C, but it VRAT is positive for clouds

Cloud test

$$VRAT = (\rho^s(blue=band1) - 0.5.\rho^s(Red=band3)) > 0.08$$

BTT=Brightness Temperature (Band 6) < Air temp(NCEP)-20 [Degree Celsius]

$$RT = \rho^s(band\ 3) > 0.4 \text{ or } \rho^s(band\ 4) > 0.6$$

$$SRT = 0.9 < (\rho^s(band\ 4) / \rho^s(band\ 3)) < 1.3$$

Another test is also added to reject any possible unfiltered water pixel or pixel contaminated by shadow, it uses the band 7 reflectance and requires that the selected pixels have a reflectance > 0.03.

Vermote et. al (2007)

Snow test

$$NDSI=(\rho^s(band2)-\rho^s(band5))/(\rho^s(band2)+\rho^s(band5)) > 0.3$$
AND
Brigthness Temperature > 280 Kelvin
AND
$$\rho^s(band4) > 0.2$$

Vermote et. al (2007)

Cloud Shadow test
Global Surface

Cloud Altitude = (air temperature-Brighthness Temperature (band6))/ **CF**

Vermote et. al (2007)

CBERS-4

BCG - Boletim de Ciências Geodésicas - On-Line version, ISSN 1982-2170
http://dx.doi.org/10.1590/S1982-21702016000200021

Artigo

DETECÇÃO AUTOMÁTICA DE NUVEM E SOMBRA DE NUVEM EM IMAGENS DE SENSORIAMENTO REMOTO

Automatic detection of cloud and cloud shadow in remote sensing images

Marco Aurélio Oliveira da Silva [1]

Frederico dos Santos Liporace [2]

[1]AMS Kepler Engenharia de Sistemas, Avenida Armando Lombardi, 800, sala 206, Barra da Tijuca - 22640-020 - Rio de Janeiro, RJ

[2]AMS Kepler Engenharia de Sistemas, Rua Alfredo Nogueira Ignácio Penido, 300, sala 58 - 12246-000 - São José dos Campos, SP

Resumo:

Nesse trabalho é apresentada uma metodologia para a detecção automática de nuvem e sombra de nuvem em imagens de sensores que atuam na faixa do visível e do infravermelho próximo. O trabalho visa à detecção em imagens do sensor AWFI que estará a bordo do satélite AMAZONIA-

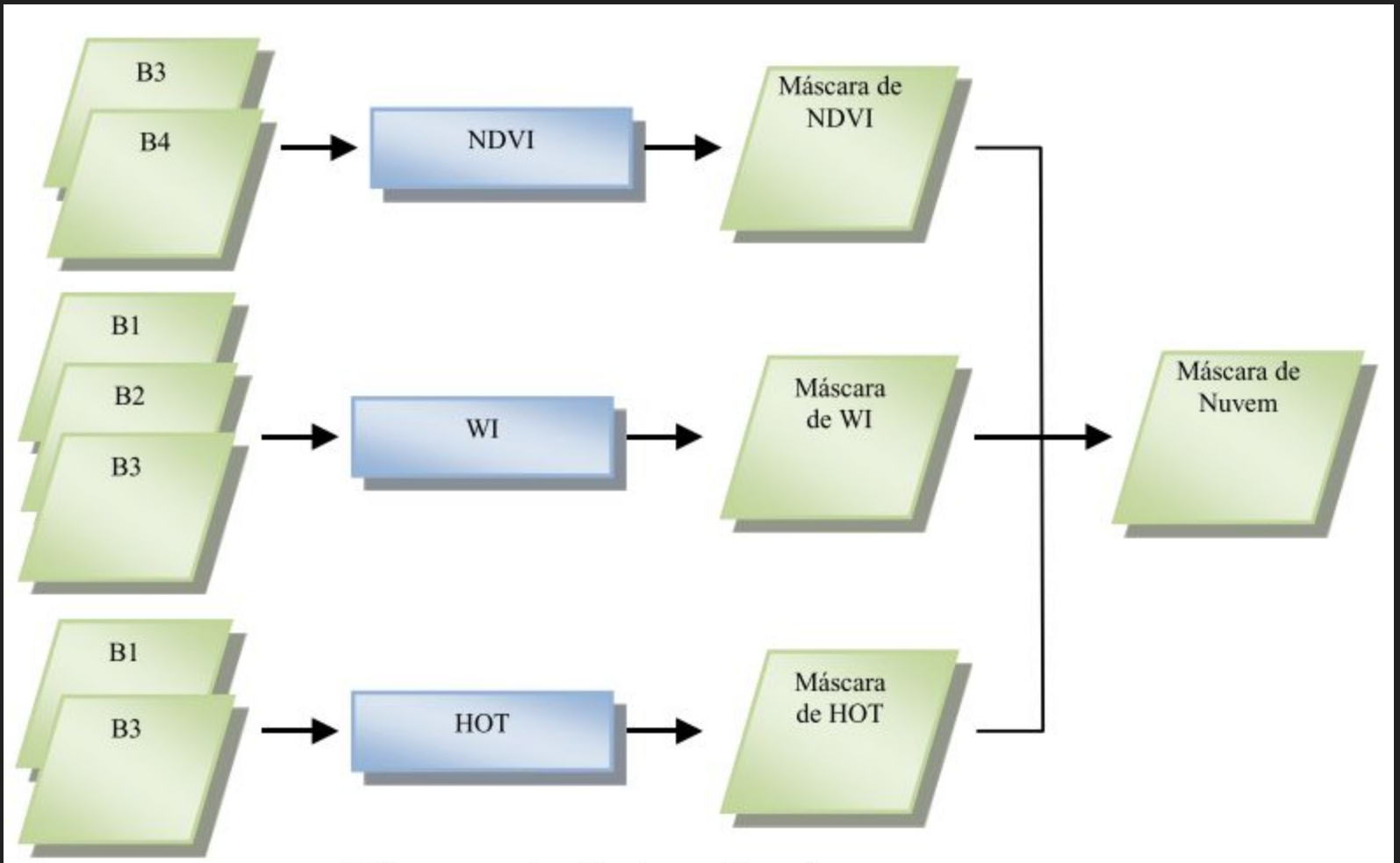

Figura 1: Detecção de nuvem.

Silva et. al (2016)

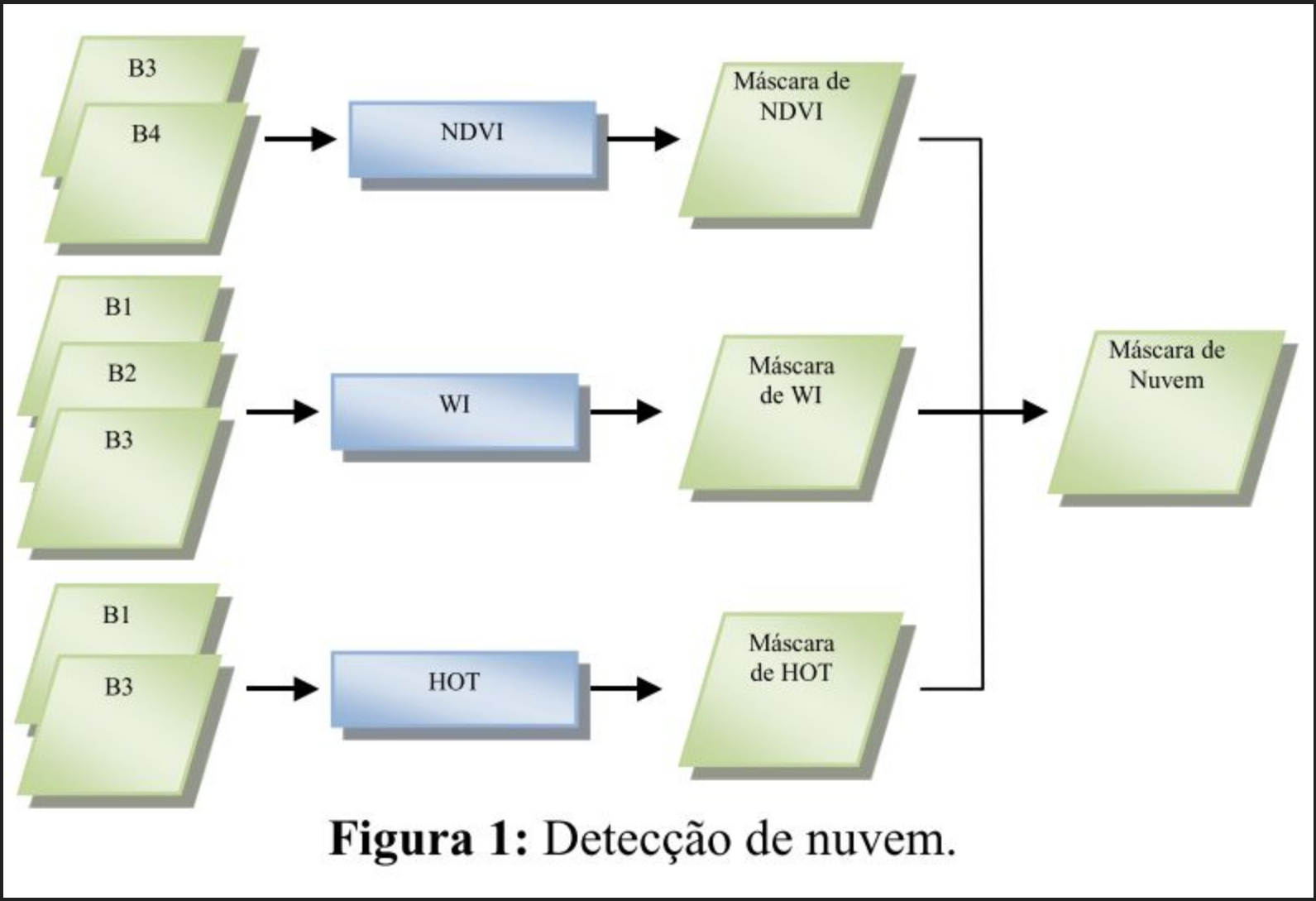

Figura 1: Detecção de nuvem.

$$NDVI_{\min} < NDVI < NDVI_{\max}$$

Silva et. al (2016)

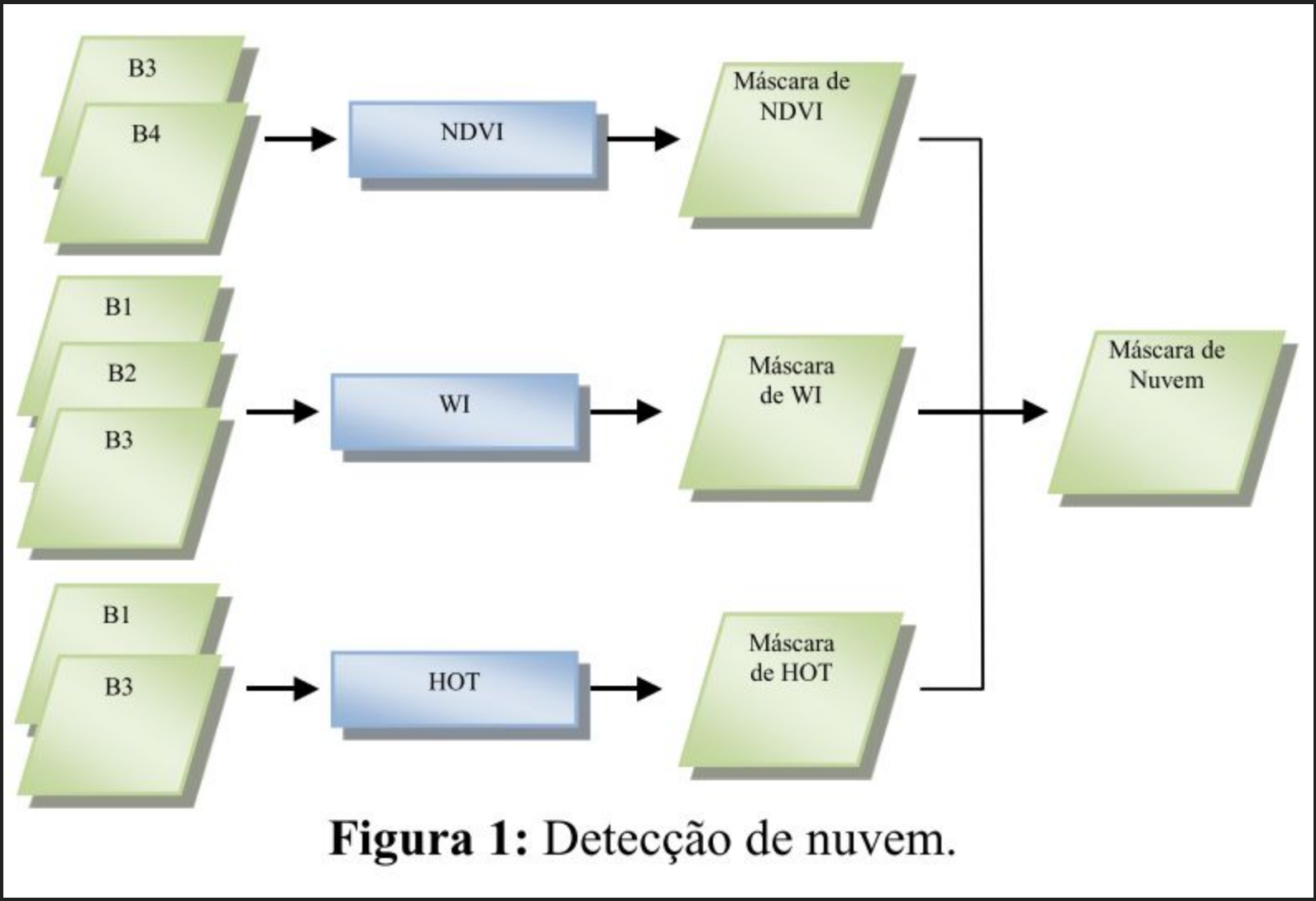

Figura 1: Detecção de nuvem.

$$NDVI_{\min} < NDVI < NDVI_{\max}$$

$$M = 0.25 \cdot B1 + 0.375 \cdot B2 + 0.375 \cdot B3$$

$$WI = \sum_{i=1}^{3} \left| \frac{Bi - M}{M} \right| < WI_{\max}$$

Silva et. al (2016)

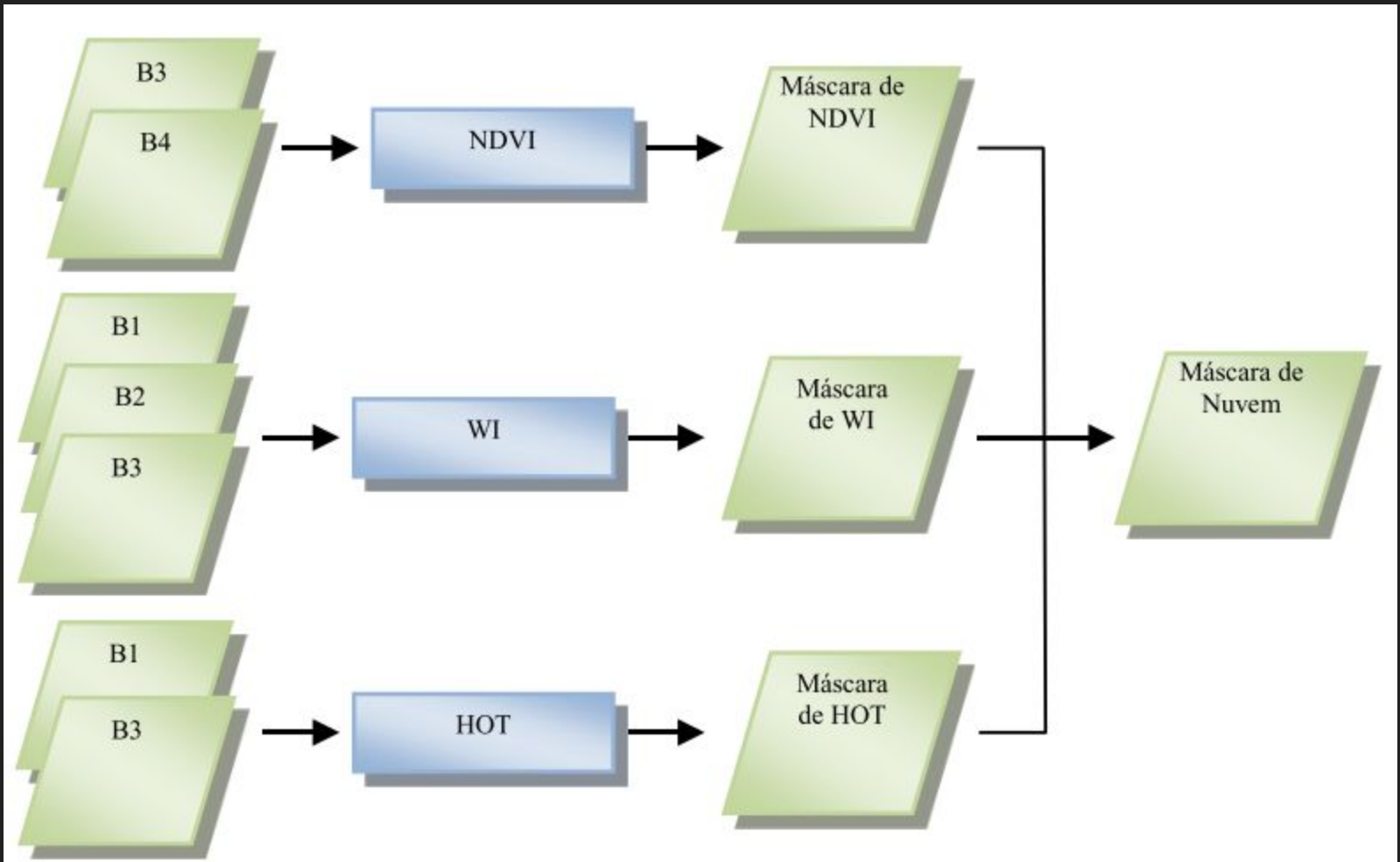

Figura 1: Detecção de nuvem.

$$NDVI_{min} < NDVI < NDVI_{max}$$

$$M = 0.25 \cdot B1 + 0.375 \cdot B2 + 0.375 \cdot B3$$

$$WI = \sum_{i=1}^{3} \left| \frac{Bi - M}{M} \right| < WI_{max}$$

$$HOT = B1 - 0.45 \cdot B3 - 0.08 > HOT_{min}$$

Silva et. al (2016)

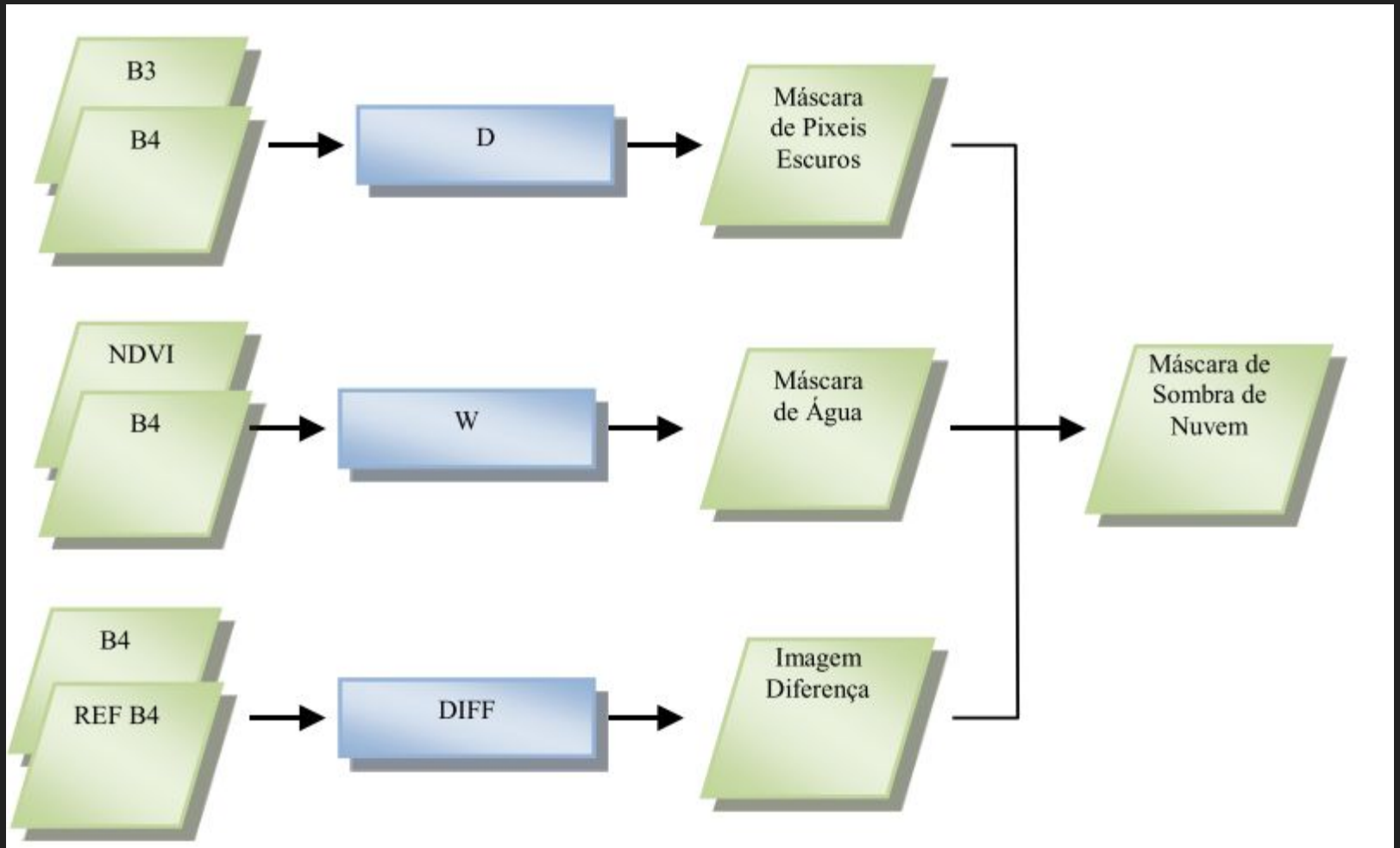

Figura 2: Detecção de sombra de nuvem.

Silva et. al (2016)

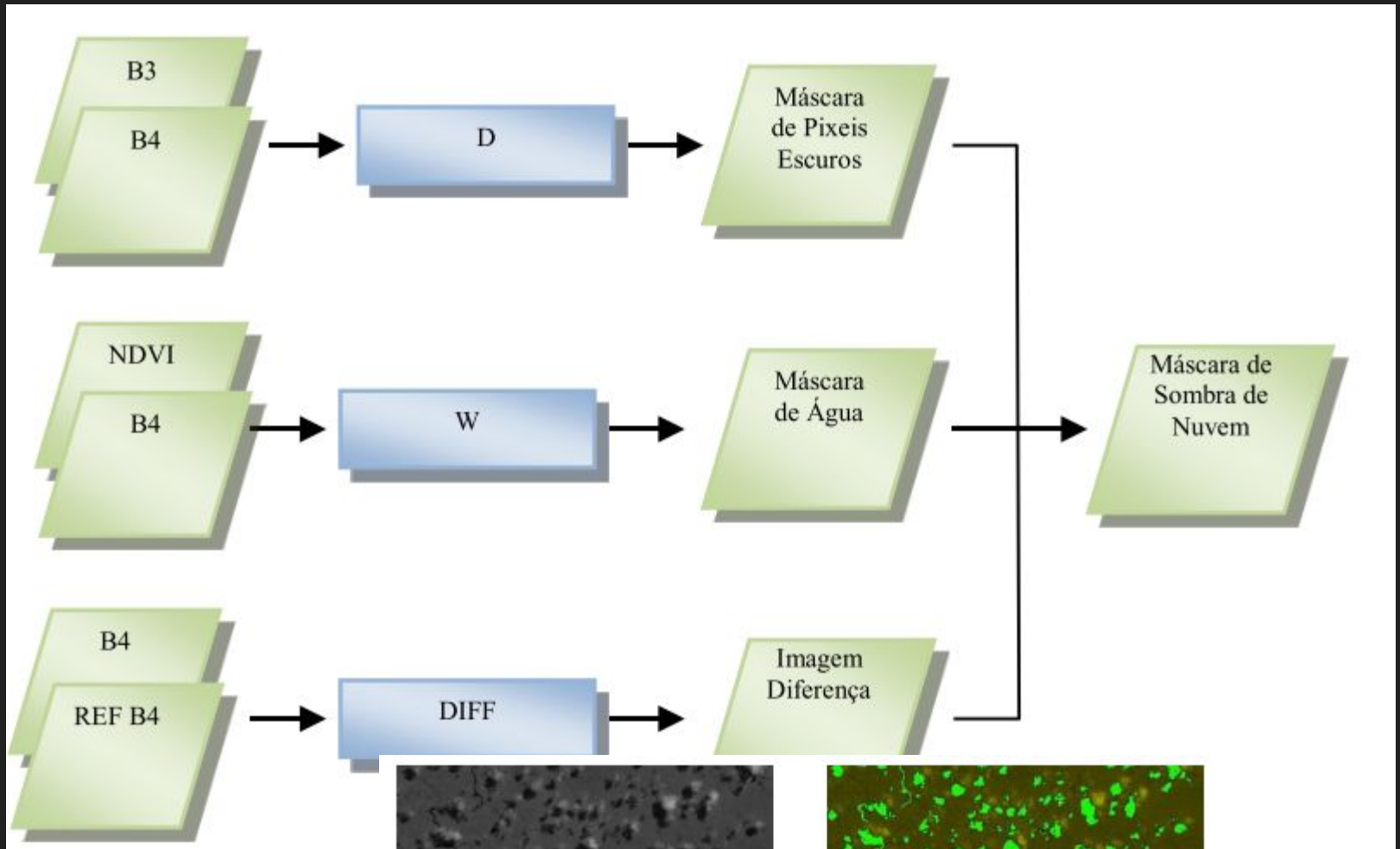

Figura

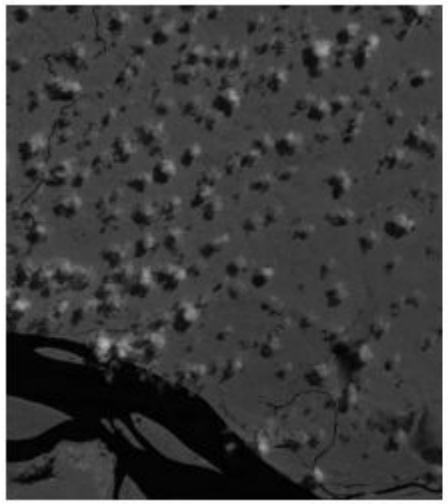

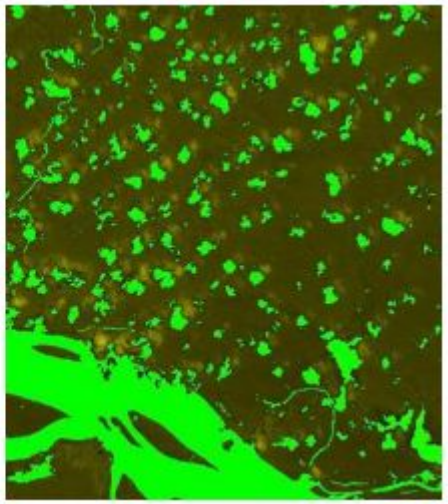

$$D_2 = B2 < (B2_{\min} + \rho_{\lambda 2})$$
$$D_4 = B4 < (B4_{\min} + \rho_{\lambda 4})$$
$$D = B2 \; and \; B4$$

Silva et. al (2016)

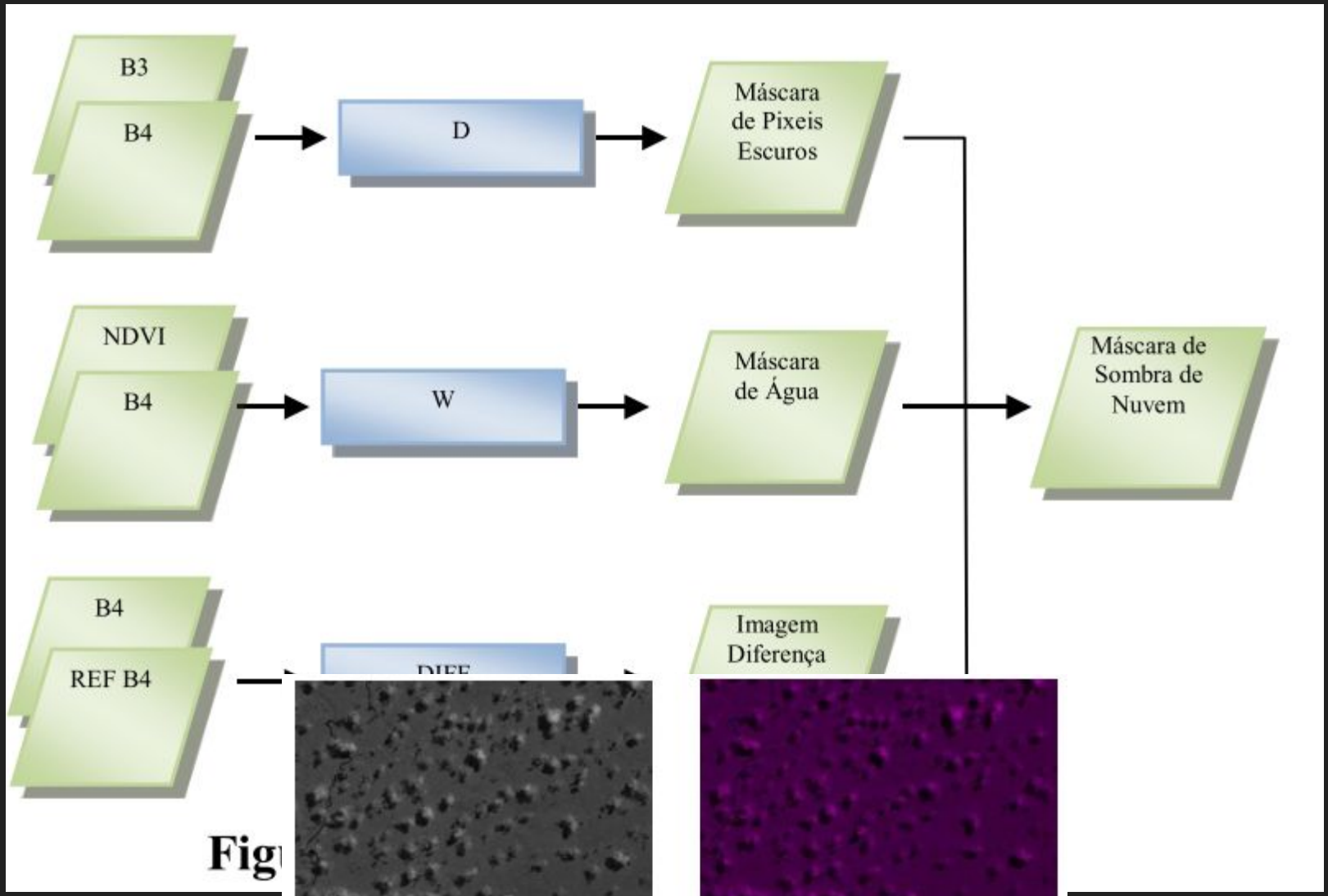

$$W = (NDVI < NDVI_{clean} \text{ and } B4 < \rho_{\lambda clean}) \text{ or } (NDVI < NDVI_{turbid} \text{ and } B4 < \rho_{\lambda turbid})$$

Silva et. al (2016)

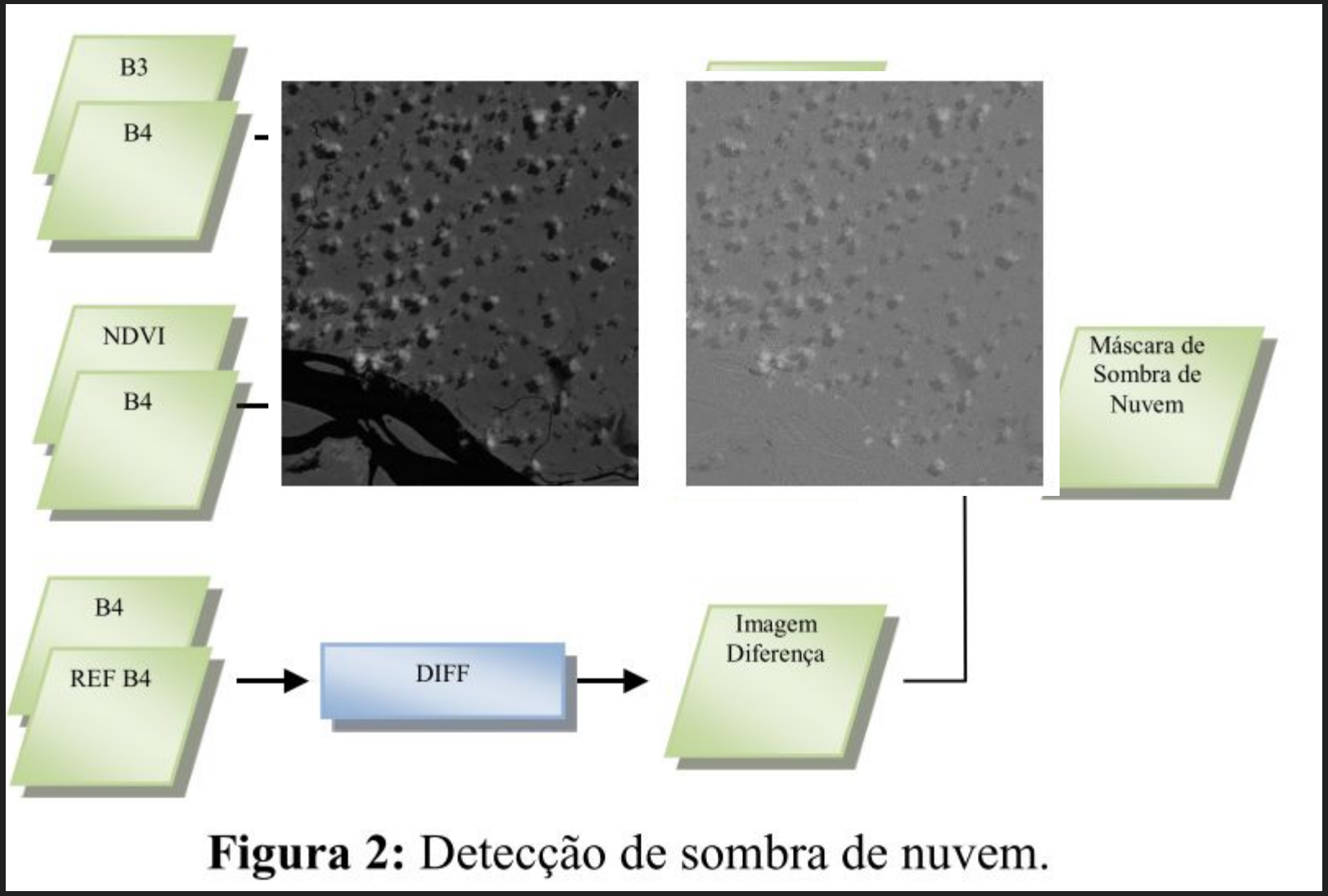

Figura 2: Detecção de sombra de nuvem.

$$DIFF = B4 - REF\ B4$$

Silva et. al (2016)

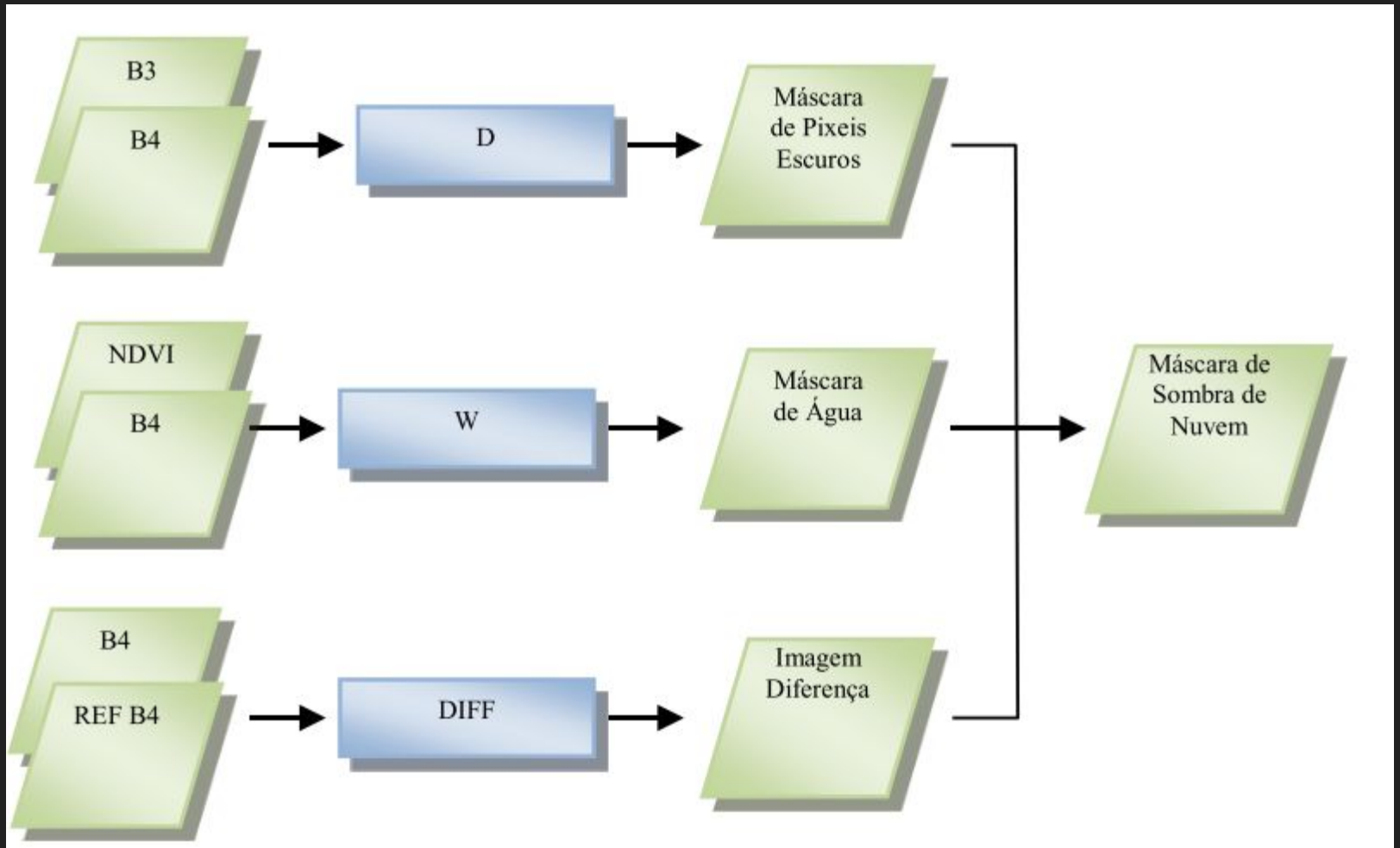

Figura 2: Detecção de sombra de nuvem.

$$CS = D \; and \; NOT(W) \; and \; (DIFF < DIFF_{\min})$$

Silva et. al (2016)

Anais do XVIII Simpósio Brasileiro de Sensoriamento Remoto -SBSR
ISBN: 978-85-17-00088-1
28 a 31 de Maio de 2017
INPE Santos - SP, Brasil

CBERS-4/MUX automatic detection of clouds and cloud shadows using decision trees

Rennan de Freitas Bezerra Marujo[1]
Leila Maria Garcia Fonseca[1]
Thales Sehn Körting[1]
Rafael Duarte Coelho dos Santos[1]
Hugo do Nascimento Bendini[1]

[1] Instituto Nacional de Pesquisas Espaciais – INPE
Caixa Postal 515 – 12245-970 – São José dos Campos - SP, Brasil
{rennan.marujo, leila.fonseca, thales.korting, rafael.santos, hugo.bendini}@inpe.br

Abstract. Cloud contamination can compromise surface observation on satellite images and impossibility land cover and land use mapping, due to their high reflectance. Similarly, cloud shadows can darken the image or be confused with water, making it harder to differentiate targets. This paper aims at evaluating an automatic cloud and cloud shadow detection method using decision tree classifier for CBERS-4 (China Brazil Earth Resources Satellite) MUX (Multispectral Camera) camera. In relation to the features used in the classification process, 3 methods were tested to classify 10 images of CBERS-4 MUX camera. The first one used spectral information and spectral indices, such as NDVI, WI and HOT; the second one added shape attributes in the feature set, and the third one added texture attributes. The classification process considered 3 classes: cloud, cloud shadow and cloud-free, which were validated using visually interpreted images. The results presented an overall accuracy of about 92.98%. The accuracy for the cloud detection was 0.91, while for the cloud shadow the classification accuracy was 0.67. These results point out that for sensors that has only visible and near infrared spectral bands, like CBERS-4/MUX, the NDVI, WI and HOT spectral indices are relevant for cloud detection. On the other hand, for cloud shadow detection it is necessary to explore other features capable to discriminate it from dark objects in the images.

Keywords: remote sensing, cloud detection, CBERS-4 .

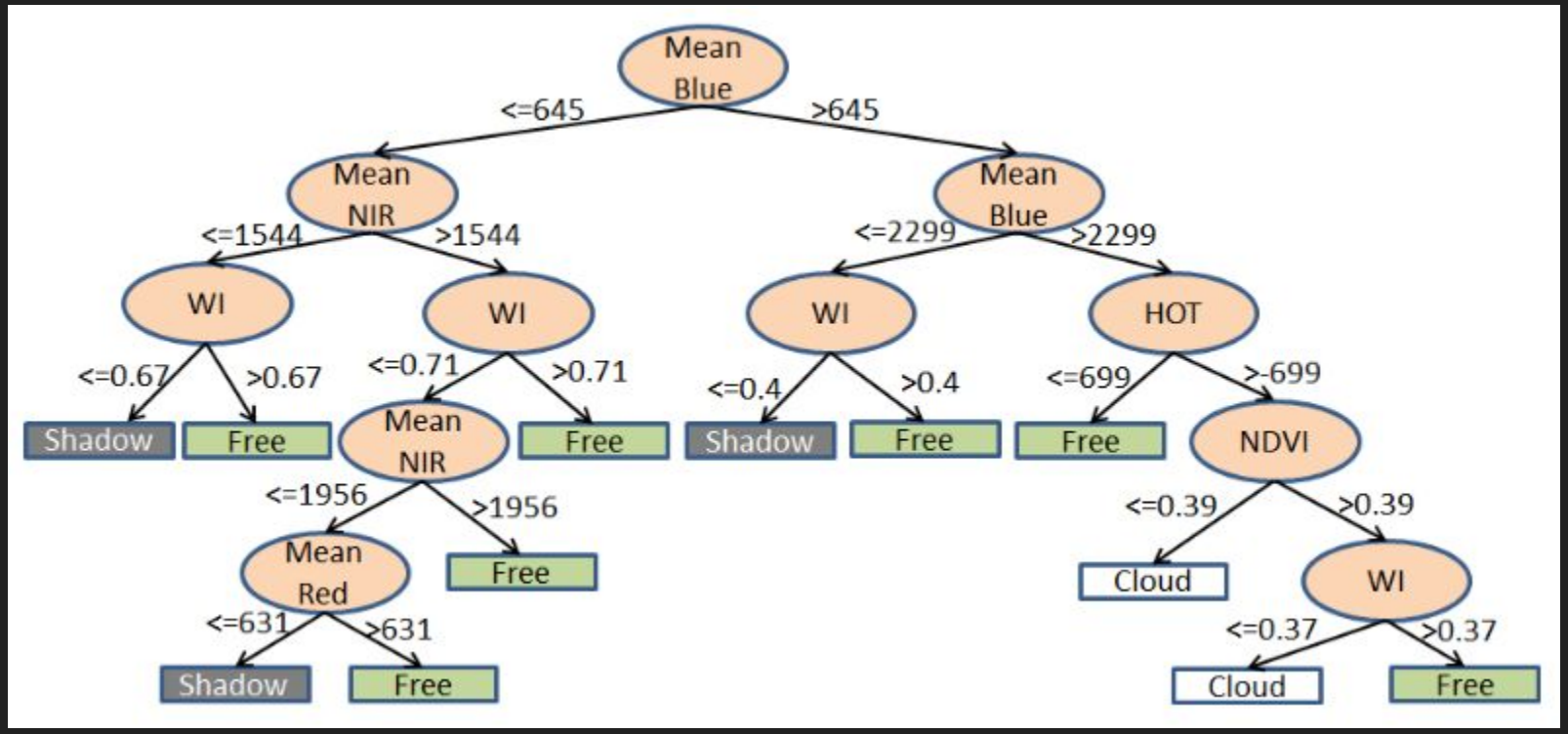

Marujo et. al (2017)

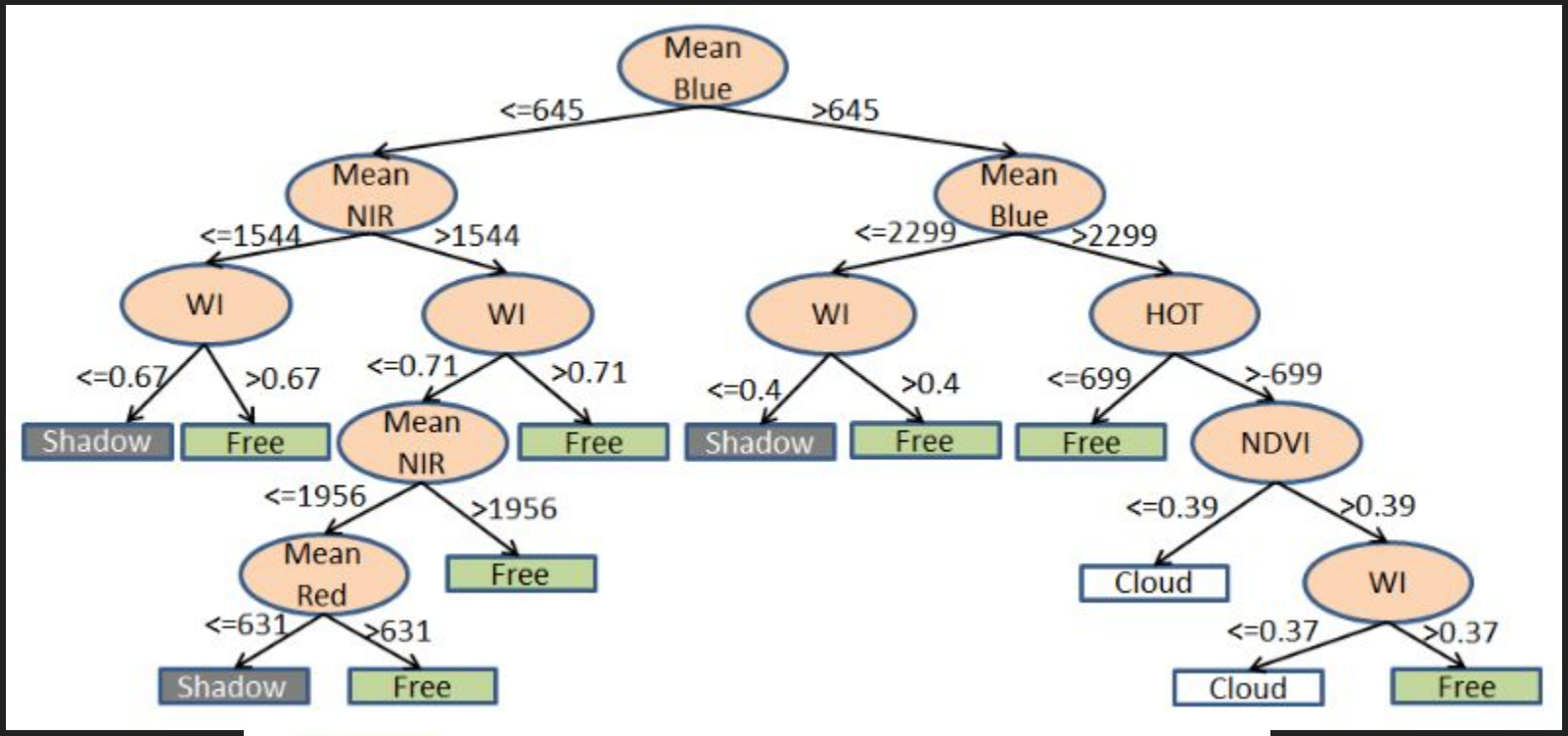

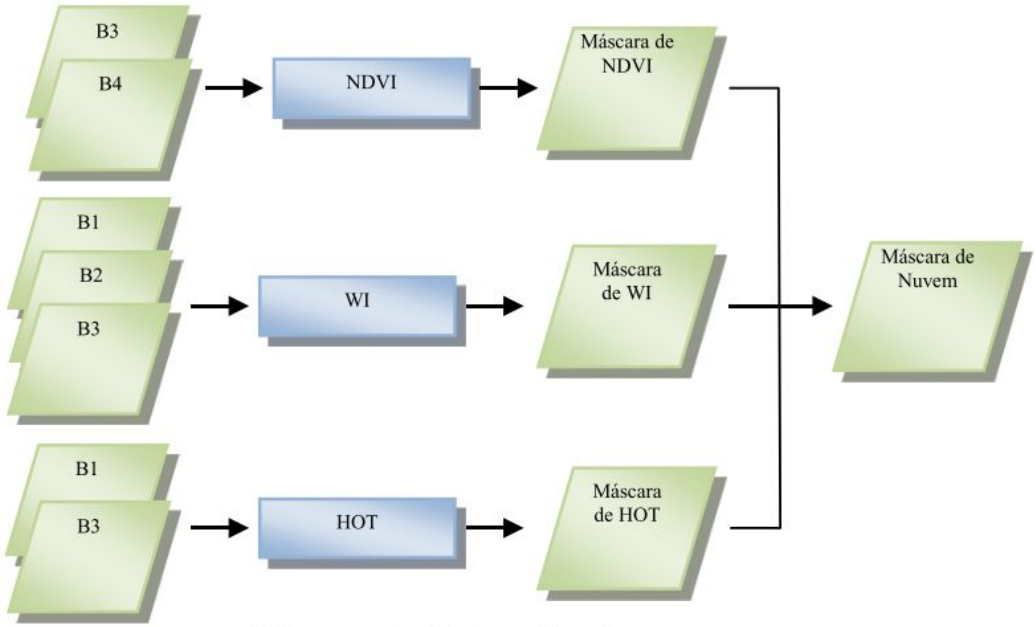

Figura 1: Detecção de nuvem.

Marujo et. al (2017)

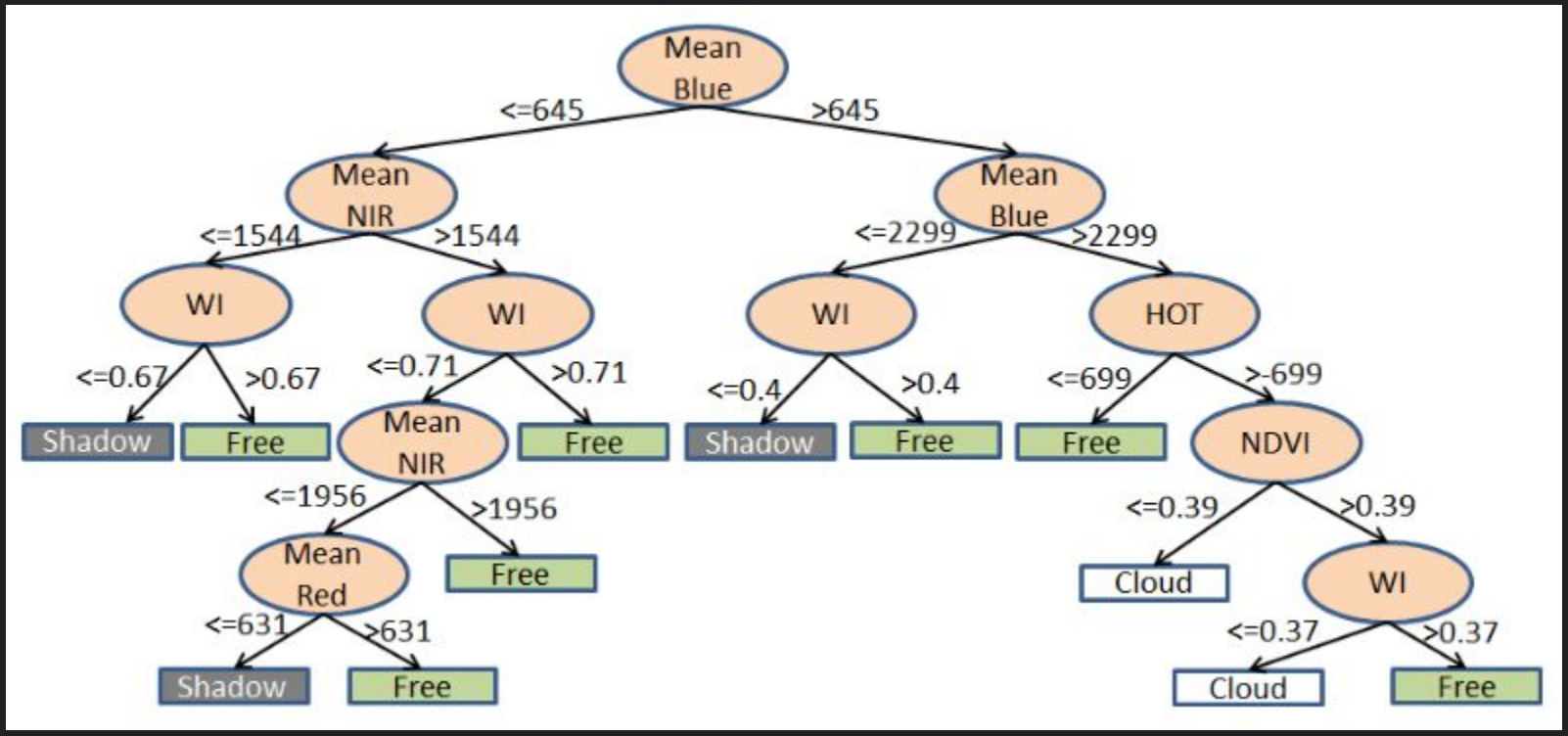

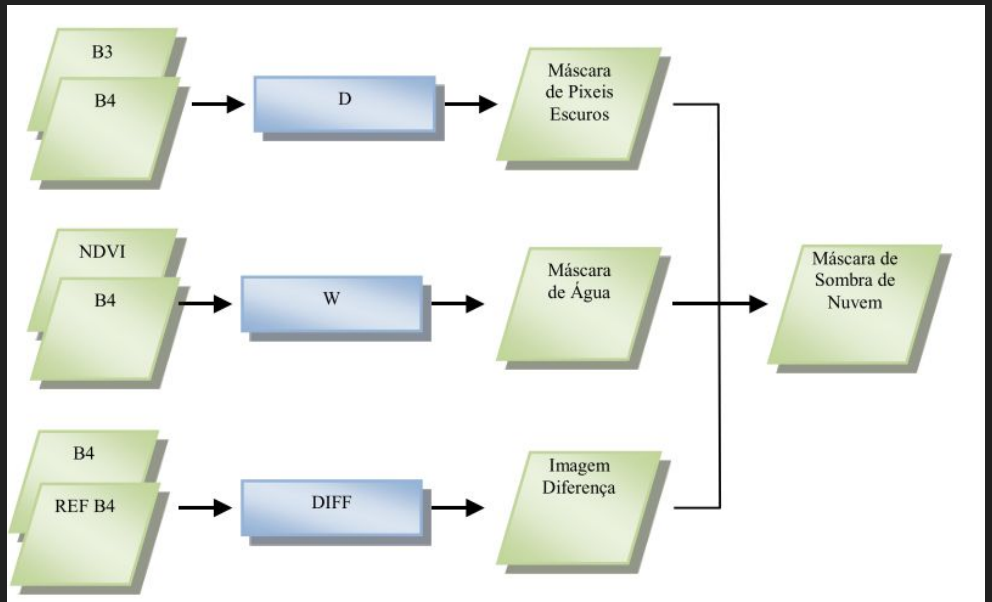

Figura 2: Detecção de sombra de nuvem.

Marujo et. al (2017)

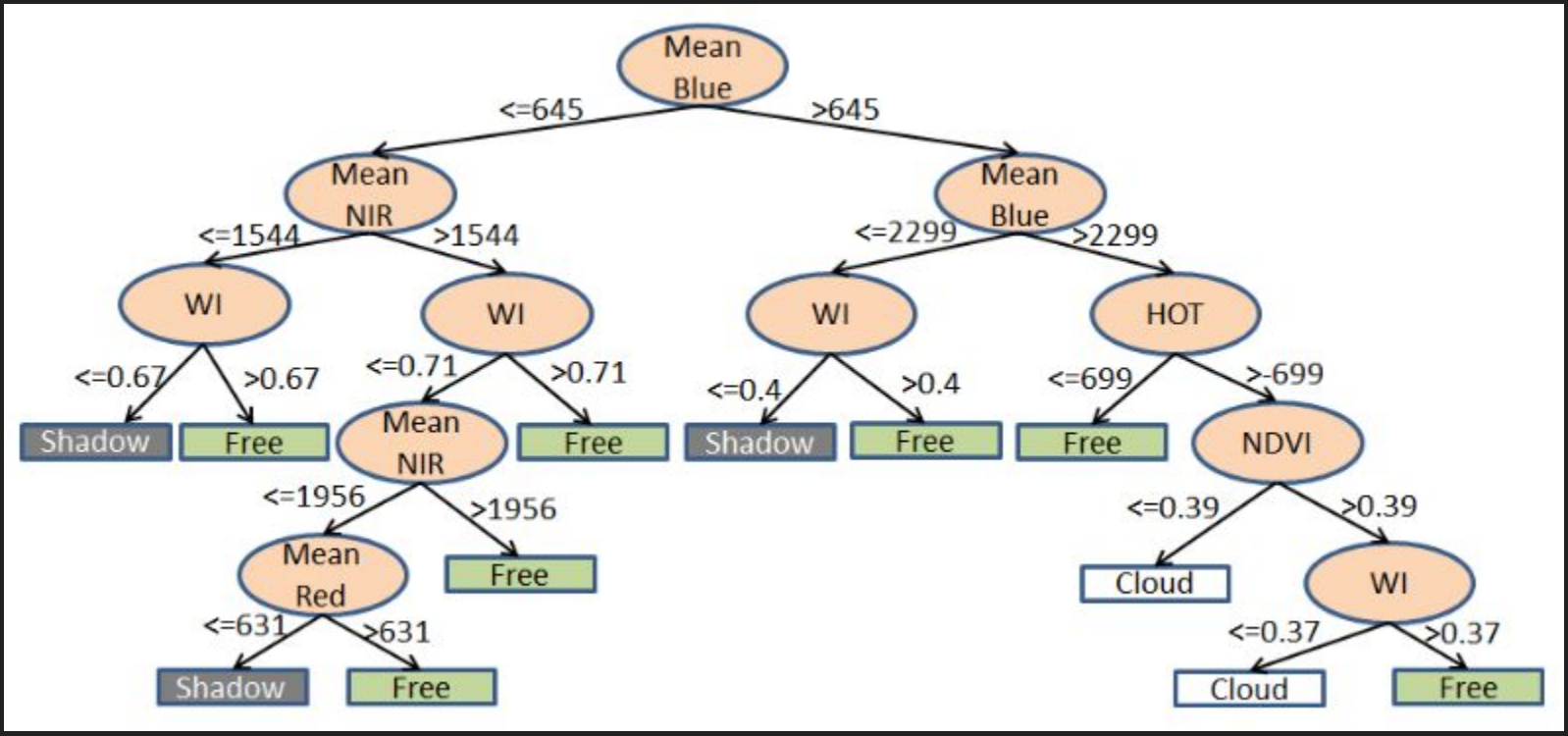

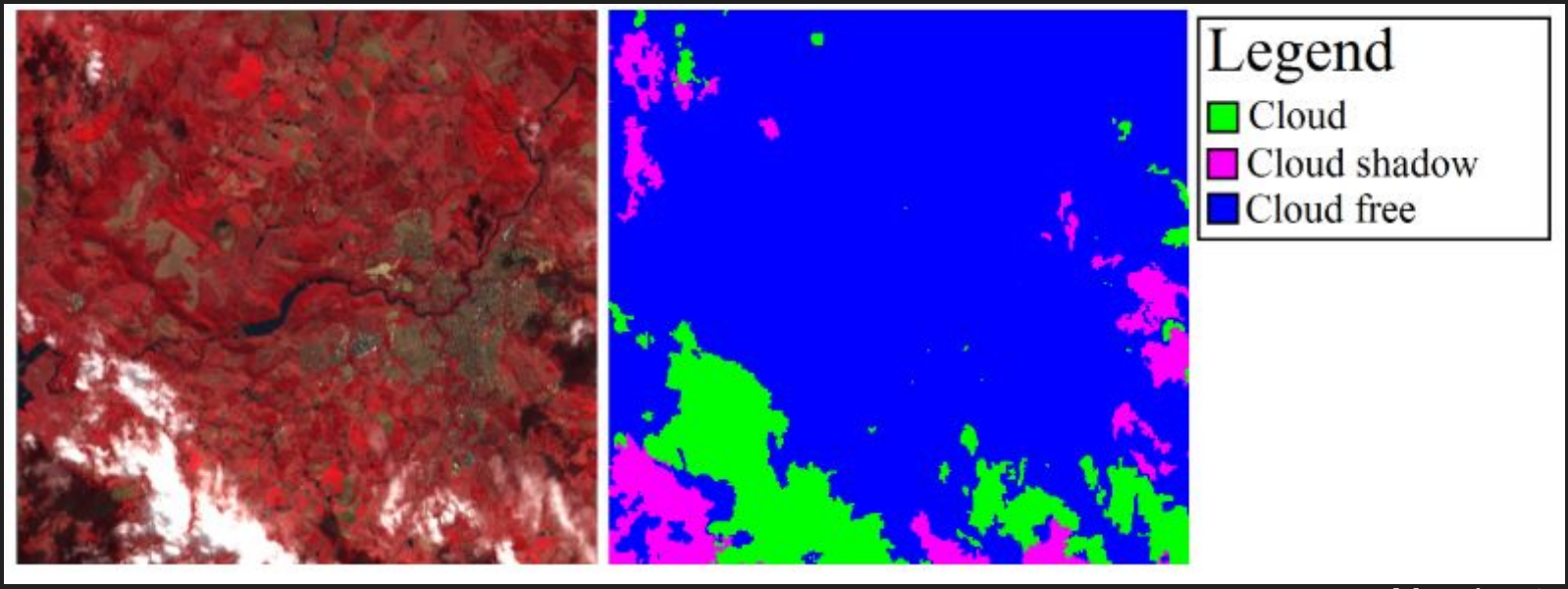

Marujo et. al (2017)

Sen2cor

Customer	:	**ESRIN**	**Document Ref**	:	**S2PAD-ATBD-0001**
Contract No	:	**21450/08/I-EC**	**Issue Date**	:	**13 April 2011**
WP No	:	**1.1.5.1.2**	**Issue**	:	**1.8**

Title : **Sentinel-2 MSI – Level 2A Products Algorithm Theoretical Basis Document**

Abstract : This document is the ATBD for Level 2A processing.

Authors : R. Richter (DLR), J. Louis, B. Berthelot (VEGA France)

Approval :

Prime Approval : Marc Niezette
Project Manager

Accepted : Christine Dingeldey
Quality Assurance Manager

Distribution :

Hard Copy File:
Filename: S2PAD-VEGA-ATBD-0001-1_8-L2A_ATBD.doc

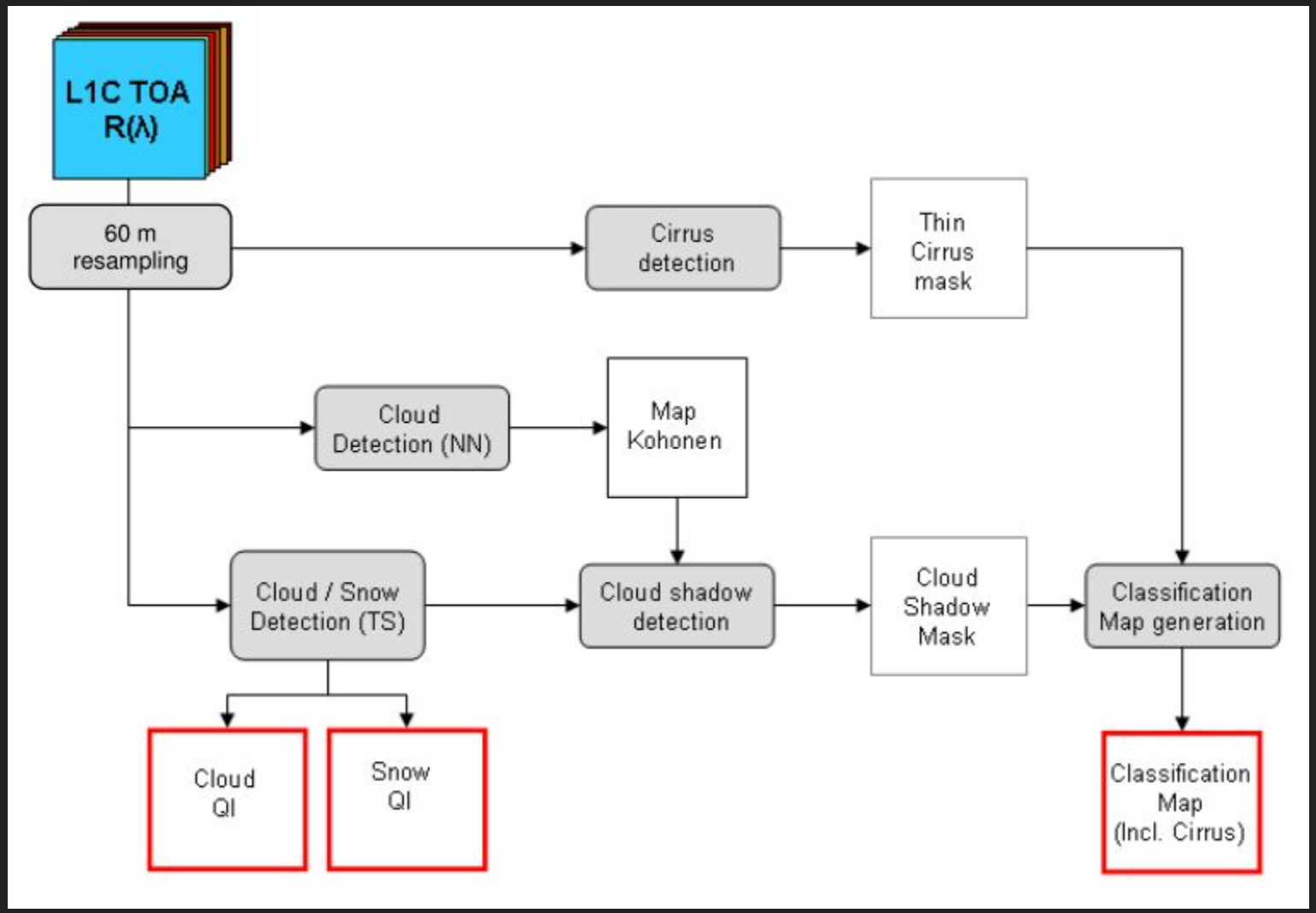

Richter et. al (2012)

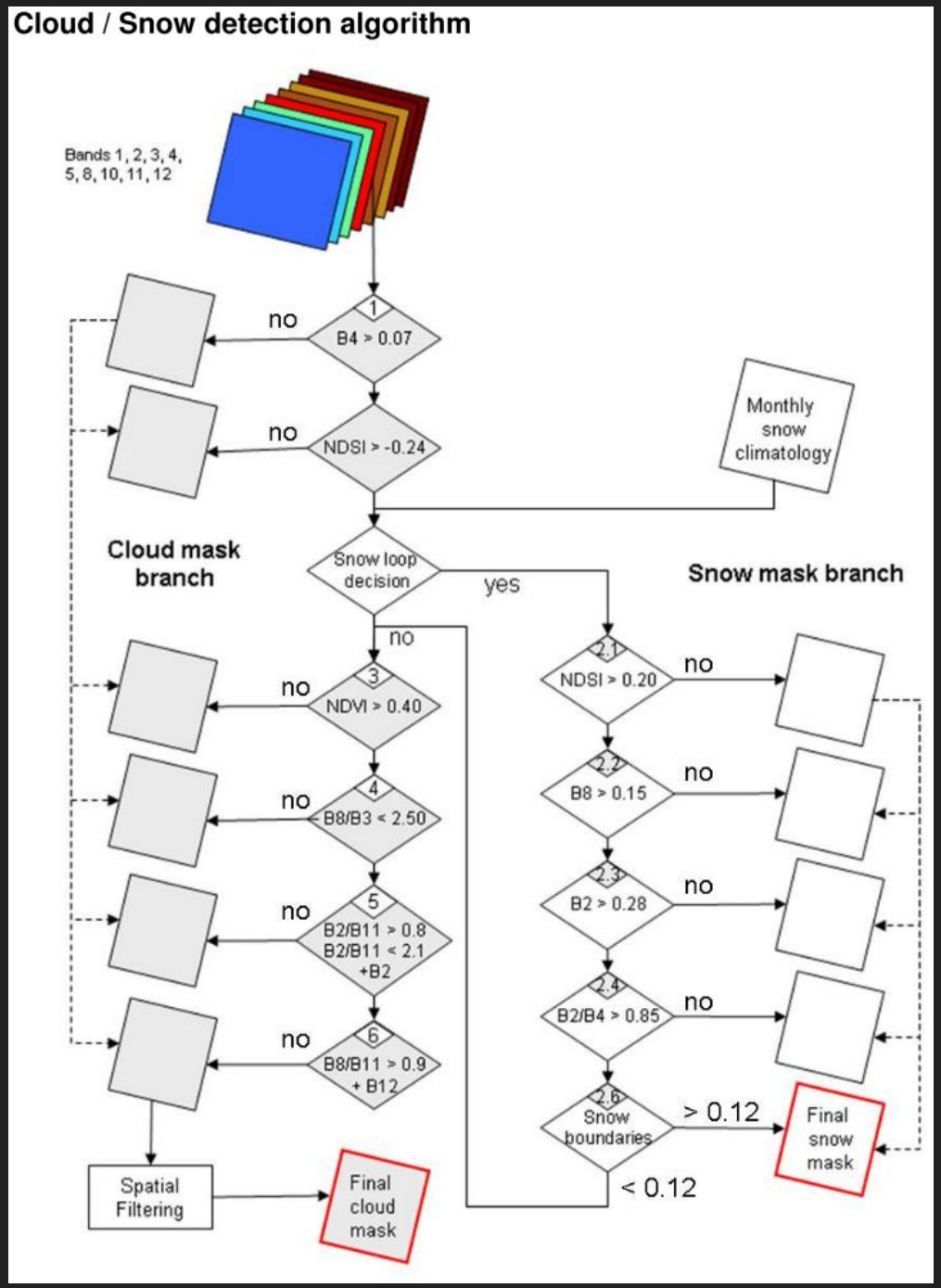

Richter et. al (2012)

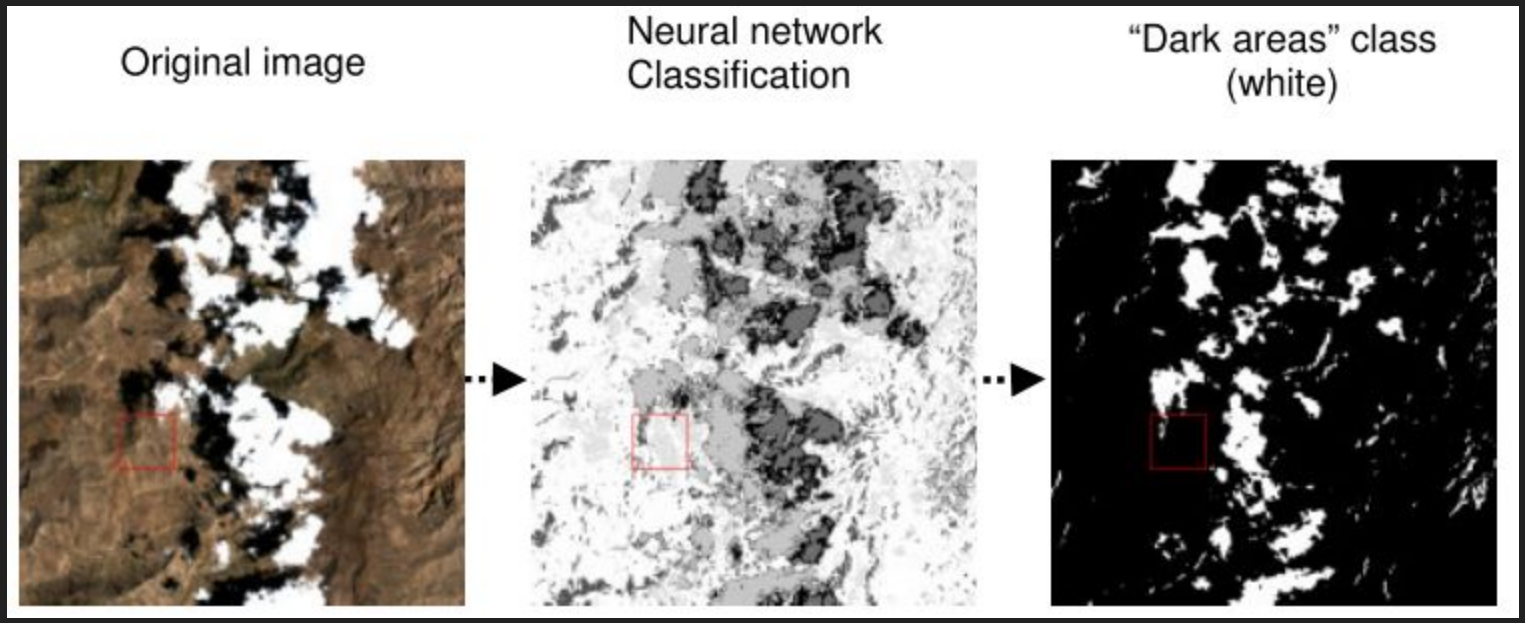

Richter et. al (2012)

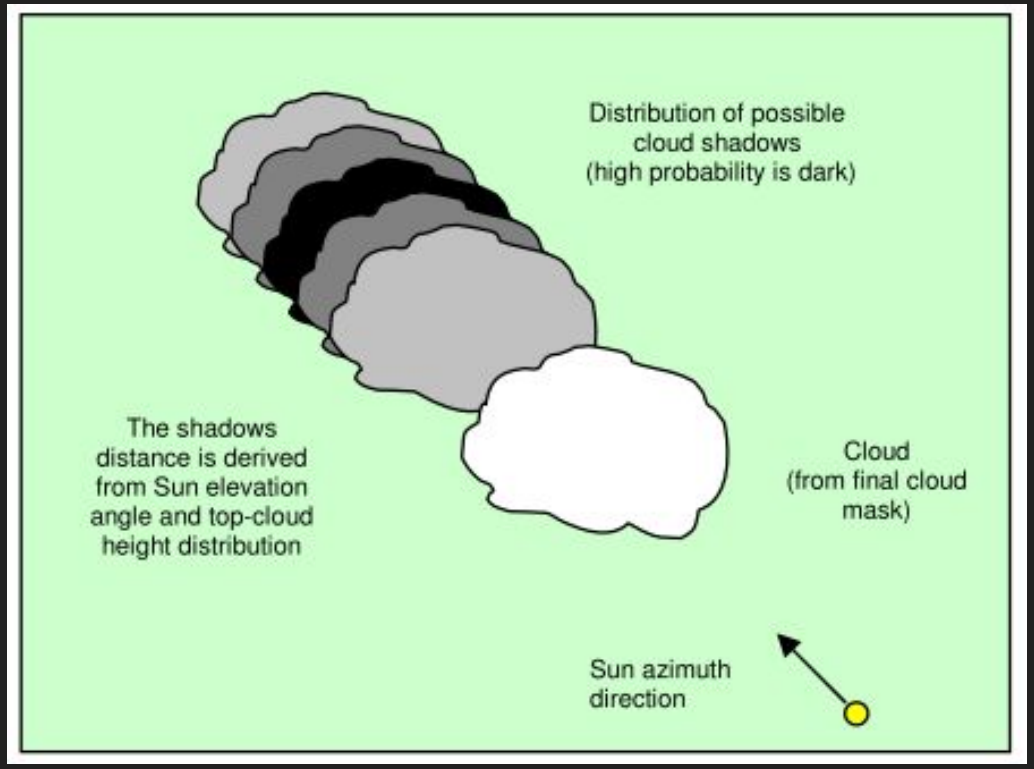

Richter et. al (2012)

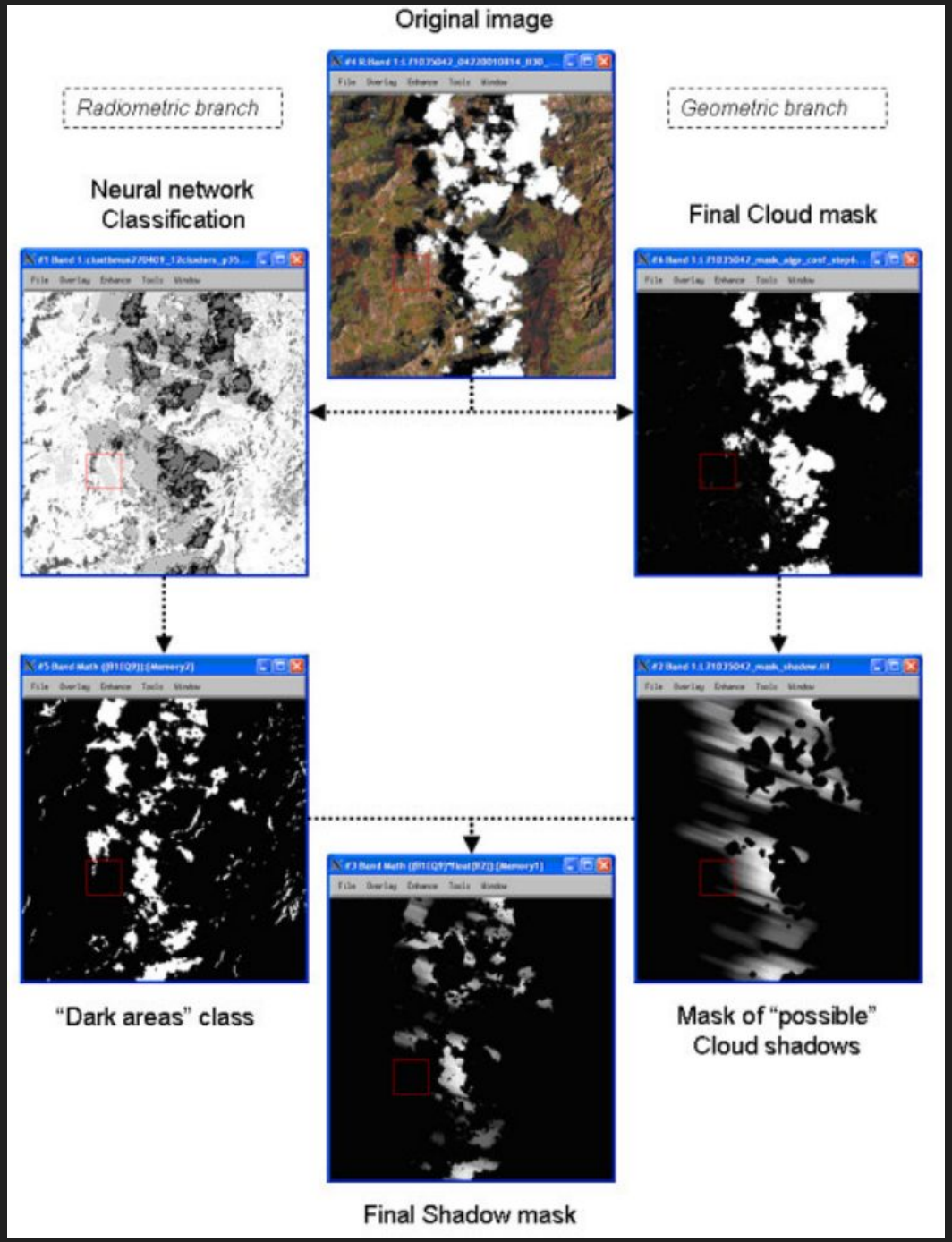

Richter et. al (2012)

FMask 4.0 (2019)

Remote Sensing of Environment 231 (2019) 111205

Contents lists available at ScienceDirect

Remote Sensing of Environment

journal homepage: www.elsevier.com/locate/rse

Fmask 4.0: Improved cloud and cloud shadow detection in Landsats 4–8 and Sentinel-2 imagery

Shi Qiu[a,c], Zhe Zhu[b,c,*], Binbin He[a,d,**]

[a] School of Resources and Environment, University of Electronic Science and Technology of China, Chengdu, Sichuan 611731, China
[b] Department of Natural Resources and the Environment, University of Connecticut, Storrs, CT 06269, USA
[c] Department of Geosciences, Texas Tech University, Lubbock, TX 79409, USA
[d] Center for Information Geoscience, University of Electronic Science and Technology of China, Chengdu, Sichuan 611731, China

ARTICLE INFO

Edited by Menghua Wang

Keywords:
Cloud
Cloud shadow
Landsat
Sentinel-2
Auxiliary data
Spectral-contextual
New cloud probability

ABSTRACT

We developed the Function of mask (Fmask) 4.0 algorithm for automated cloud and cloud shadow detection in Landsats 4–8 and Sentinel-2 images. Three major innovative improvements were made as follows: (1) integration of auxiliary data, where Global Surface Water Occurrence (GSWO) data was used to improve the separation of land and water, and a global Digital Elevation Model (DEM) was used to normalize thermal and cirrus bands; (2) development of new cloud probabilities, in which a Haze Optimized Transformation (HOT)-based cloud probability was designed to replace temperature probability for Sentinel-2 images, and cloud probabilities were combined and re-calibrated for different sensors against a global reference dataset; and (3) utilization of spectral-contextual features, where a Spectral-Contextual Snow Index (SCSI) was created for better distinguishing snow/ice from clouds in polar regions, and a morphology-based approach was applied to reduce the commission error in bright land surfaces (e.g., urban/built-up and mountain snow/ice). The Fmask 4.0 algorithm showed higher overall accuracies for Landsats 4–8 imagery than the 3.3 version (Zhu et al., 2015) (92.40% versus 90.73% for Landsats 4–7 and 94.59% versus 93.30% for Landsat 8), and much higher overall accuracies for Sentinel-2 imagery than the 2.5.5 version of the Sen2Cor algorithm (Müller-Wilm et al., 2018) (94.30% versus 87.10%).

1. Introduction

Moderate spatial resolution images (10 to 30 m) from Landsats 4–8 and Sentinel-2 provide a great opportunity for monitoring global en-

multitemporal algorithms are particularly popular after the free policy of Landsat and Sentinel-2 (Frantz et al., 2015; Goodwin et al., 2013; Hagolle et al., 2010; Wang et al., 1999; Zhu and Helmer, 2018; Zhu and Woodcock, 2014). As the presence of cloud and cloud shadow will lead

HLS

HLS cloud mask

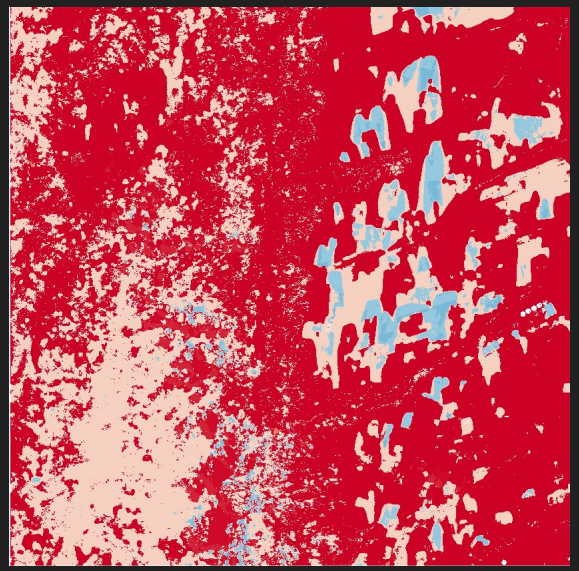

Sen2Cor cloud mask